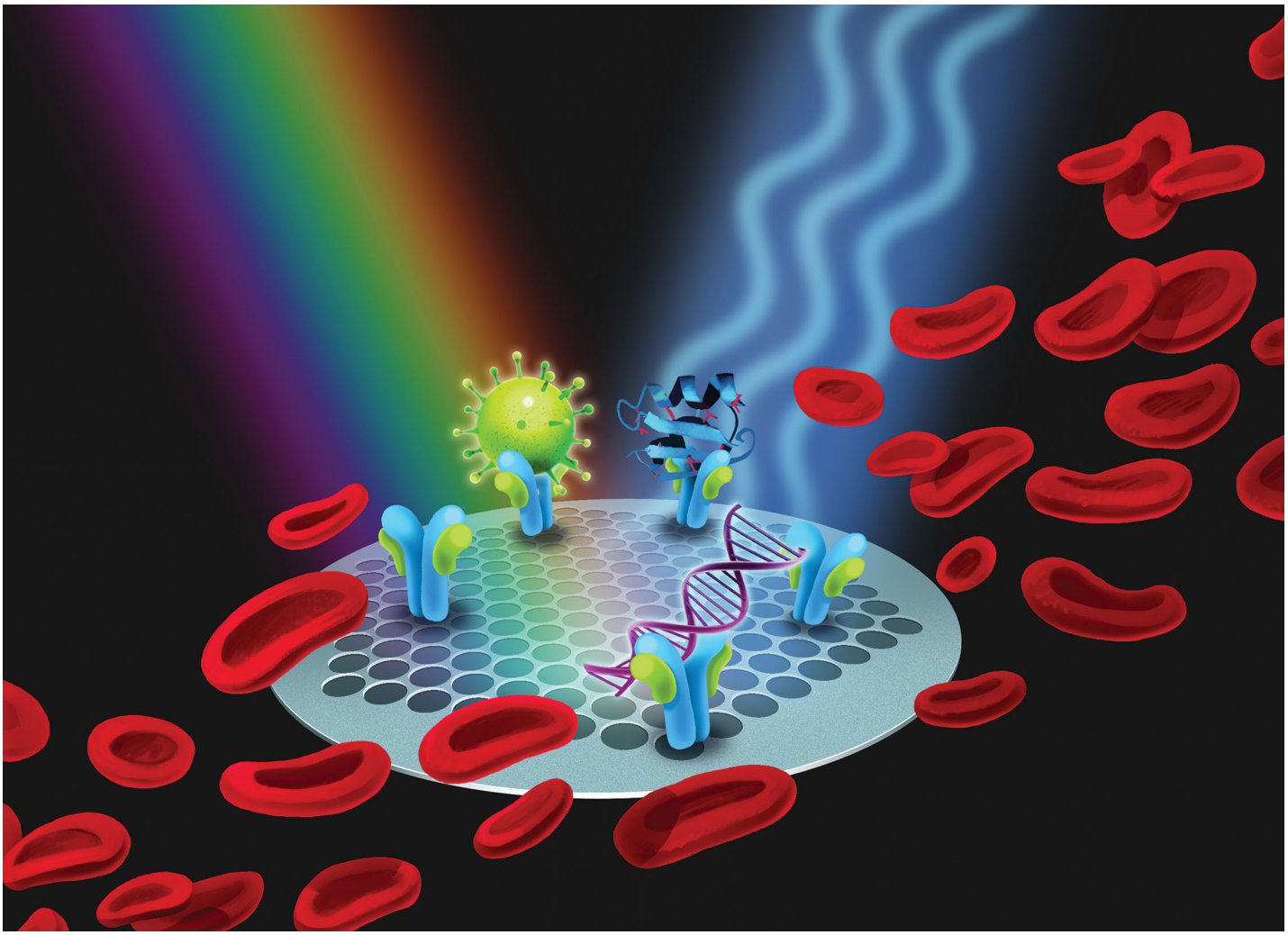

Featuring work from the research group of Professor Utkan Demirci, Stanford University School of Medicine, California, USA.

Photonic crystals: emerging biosensors and their promise for point-of-care applications

Photonic crystals integrated with emerging technologies (such as smartphones, microfluidics, and wearable and flexible materials) hold great promise for biosensing applications at point-of-care (POC).

As featured in:

See Brian T. Cunningham, Utkan Demirci *et al.*, *Chem. Soc. Rev.*, 2017, **46**, 366.

ROYAL SOCIETY OF CHEMISTRY

rsc.li/chem-soc-rev

Registered charity number: 207890

Chem Soc Rev

REVIEW ARTICLE

View Article Online
View Journal | View Issue

Cite this: *Chem. Soc. Rev.*, 2017, **46**, 366

Photonic crystals: emerging biosensors and their promise for point-of-care applications

Hakan Inan,[a] Muhammet Poyraz,[ab] Fatih Inci,[a] Mark A. Lifson,[a] Murat Baday,[a] Brian T. Cunningham*[c] and Utkan Demirci*[ad]

Biosensors are extensively employed for diagnosing a broad array of diseases and disorders in clinical settings worldwide. The implementation of biosensors at the point-of-care (POC), such as at primary clinics or the bedside, faces impediments because they may require highly trained personnel, have long assay times, large sizes, and high instrumental cost. Thus, there exists a need to develop inexpensive, reliable, user-friendly, and compact biosensing systems at the POC. Biosensors incorporated with photonic crystal (PC) structures hold promise to address many of the aforementioned challenges facing the development of new POC diagnostics. Currently, PC-based biosensors have been employed for detecting a variety of biotargets, such as cells, pathogens, proteins, antibodies, and nucleic acids, with high efficiency and selectivity. In this review, we provide a broad overview of PCs by explaining their structures, fabrication techniques, and sensing principles. Furthermore, we discuss recent applications of PC-based biosensors incorporated with emerging technologies, including telemedicine, flexible and wearable sensing, smart materials and metamaterials. Finally, we discuss current challenges associated with existing biosensors, and provide an outlook for PC-based biosensors and their promise at the POC.

Received 12th March 2016

DOI: 10.1039/c6cs00206d

www.rsc.org/chemsocrev

[a] *Demirci Bio-Acoustic-MEMS in Medicine (BAMM) Laboratory, Stanford University School of Medicine, Department of Radiology, Canary Center at Stanford for Cancer Early Detection, 3155 Porter Drive, Palo Alto, CA 94304, USA. E-mail: utkan@stanford.edu*

[b] *Department of Electrical Engineering, Stanford University, Stanford, CA, USA*

[c] *Department of Electrical and Computer Engineering, Department of Bioengineering, University of Illinois at Urbana-Champaign, Urbana, IL, USA. E-mail: bcunning@illinois.edu*

[d] *Department of Electrical Engineering (by courtesy), Stanford University, Stanford, CA, USA*

Hakan Inan

Hakan Inan is a postdoctoral research fellow at the Canary Cancer Early Detection Center at the Medicine Faculty, Stanford University. He is working on microfluidics and nanotechnology-based diagnostic devices and techniques for cancer diagnosis and prognosis for point-of-care applications. He obtained his Master and PhD degrees in nanotechnology. He joined Professor Utkan Demirci's lab at Stanford University in 2014 as a visiting graduate student and has performed his research in the same group since then. He has 12 years of teaching experience at high school and undergraduate level, where he taught chemistry and biochemistry.

Muhammet Poyraz

Muhammet Poyraz is a PhD student in electrical engineering at Stanford University and a graduate researcher at the Canary Center at Stanford for Cancer Early Detection. He received his BS degree from Bilkent University, Turkey, in electrical and electronics engineering. He joined Professor Utkan Demirci's lab at Stanford University in 2016 as a graduate student. He is currently working on photonic crystal and plasmonic based biosensing technologies for point-of-care applications.

1. Introduction

Biosensing is an emerging analytical field for the detection of biochemical interactions leveraging electrical, optical, calorimetric, and electrochemical transducing systems.[1,2] These transduction mechanisms are employed to translate changes and variations within the biological domain into a readable and quantifiable signal (*e.g.*, association, dissociation, and oxidation).[3] Biosensors are most notably employed for detecting various biological targets,

Fatih Inci

Fatih Inci received the PhD degree from Istanbul Technical University (Turkey), focusing on biosensor design and development for clinical and pharmaceutical applications. He was then appointed as a Postdoctoral Research Fellow at Harvard Medical School and Stanford University School of Medicine. Dr Inci is currently working as a Basic Life Science Research Scientist at Stanford University School of Medicine, Canary Center at Stanford for Cancer Early Detection. His research is focused on creating point-of-care diagnostic technologies, lab-on-a-chip platforms, nanoplasmonic biosensors, and surface chemistry approaches for medical diagnostics. Dr Inci's work has been highlighted in the NIH–NIBIB, Boston University, Canary Center at Stanford, Johns Hopkins University, JAMA, Nature Medicine, AIP, Newsweek, and Popular Science.

Mark A. Lifson

Mark Lifson is a biomedical and computer engineer currently working as a postdoctoral research fellow at Stanford. He obtained his Bachelor of Science in computer engineering from the Rochester Institute of Technology, and his Master of Science and Doctorate from the University of Rochester in biomedical engineering. His research interests include developing ultra-sensitive sensors for biomarker detection. He has expertise in photonic crystals, microfluidics, localized surface plasmon resonance, and smart colloidal nanoparticles.

Brian T. Cunningham

Brian T. Cunningham is the Willett Professor of Engineering in the Department of Electrical and Computer Engineering at the University of Illinois at Urbana-Champaign, where he also serves as the Director of the Micro and Nanotechnology Laboratory. His research interests include the development of biosensors and detection instruments for pharmaceutical high throughput screening, disease diagnostics, point-of-care testing, life science research, and environmental monitoring. He has published 160 peer-reviewed journal articles, and is an inventor on 83 patents. Prof. Cunningham was a co-founder of SRU Biosystems in 2000, and founded Exalt Diagnostics in 2012 to commercialize photonic crystal enhanced fluorescence technology for disease biomarker detection. Acoustic MEMS biosensor technology that he developed at the Draper Laboratory has been commercialized by Bioscale, Inc. Prof. Cunningham's work was recognized with the IEEE Sensors Council Technical Achievement Award and the IEEE Engineering in Medicine and Biology Technical Achievement Award. He is a member of the National Academy of Inventors and a Fellow of IEEE, OSA, and AIMBE.

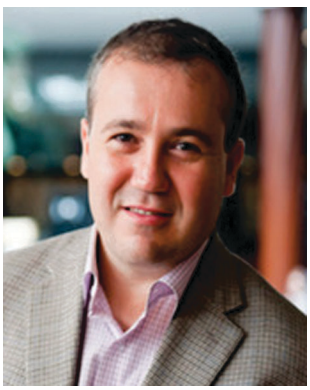

Utkan Demirci

Utkan Demirci is an Associate Professor at the School of Medicine, Department of Radiology, Canary Center at Stanford for Cancer Early Detection. His research interests involve the applications of microfluidics, nanoscale technologies and acoustics in medicine, especially portable, inexpensive, disposable technology platforms in resource-constrained settings for global health problems and 3-D biofabrication and tissue models including 3-D cancer and neural cultures. Dr Demirci has published over 120 peer-reviewed publications, over 150 conference abstracts and proceedings, 10 book chapters, and edited four books. His work has been recognized by numerous awards including the NSF Faculty Early Career Development (CAREER) Award and the IEEE-EMBS Early Career Achievement Award. He was selected as one of the world's top 35 young innovators under the age of 35 (TR-35) by the MIT Technology Review. His patents have been translated into start-up companies including DxNOW and Koek Biotech. Some of these technologies are clinically available across the globe.

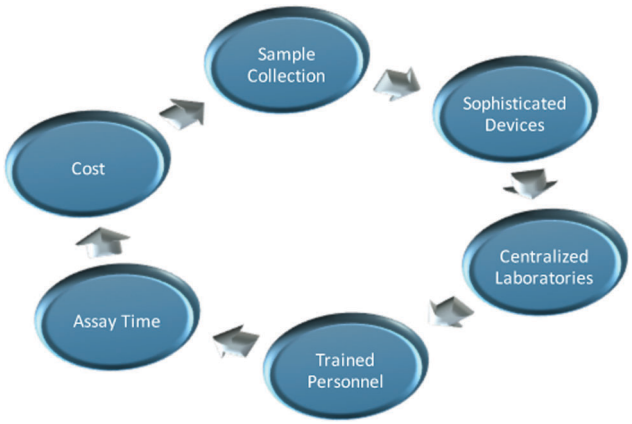

Fig. 1 Current challenges of biosensing tests for the POC applications. Biosensors face critical impediments at the POC due to large sample volume, transfer of samples to a central site, and being bulky and expensive. These challenges are most obvious at remote regions and resource-constrained settings.

such as cells,[4] bacteria,[5,6] viruses,[7] proteins,[8] hormones,[9] enzymes,[10] and nucleic acids,[11] to facilitate the diagnosis and prognosis of diseases. Currently, state of the art clinical laboratories require trained personnel to perform sample collection, testing, and analysis using sophisticated biosensing devices in centralized clinical settings (Fig. 1). Staffing the necessary personnel to ensure accurate and reliable readings can be costly, and results are subject to operator error.[12,13] Although certain automated instrumentation has been used to simultaneously process multiple patient samples at large volumes (*e.g.*, hematology analyzers), technicians are still needed for device oversight and maintenance.[14,15] Centralized laboratories also perform immunoassays and nucleic amplification strategies, but these methods are time consuming, labor intensive, and expensive. As an example, enzyme-linked immunosorbent assay (ELISA) requires several experimental steps, including antibody immobilization, target binding, labeling, substrate incubation, signal production, and multiple washing steps.[16,17]

Recently, substantial research efforts have been devoted to the development of *in vitro* diagnostic tests including point-of-care (POC) devices with the market volume estimated to reach US$ 75.1 billion by 2020.[18] One of the main drivers for these POC technologies is the detection of diseases in resource-limited countries.[19–25] For example, commercial POC kits have been recently developed to detect human immunodeficiency virus (HIV) and tuberculosis in such settings.[26] However, there are significant logistical, technical, and social barriers that need to be overcome when performing testing at these sites, and many of these technologies still require the recruitment and training of personnel (Fig. 1).[14,27–29,30] Thus, there exists a need to develop affordable, sensitive, rapid, portable, label-free, and user-friendly POC diagnostic tools.[31–33]

Incorporation of microfluidics and nanotechnology into biosensing platforms holds great promise to address the aforementioned challenges. Sensitive technologies, such as localized and surface plasmon resonance, electrical sensors, interferometric biosensors, and photonic crystal (PC)-based biosensors, have been employed as diagnostic devices (Table 1).[34–40] PC-based biosensors hold many advantages over other existing competing biosensing technologies, including cost-effective fabrication and short assay time (Table 2). PC structures have been used to detect a wide array of biotargets in biological sample matrices, such as blood, urine, sweat, and tears,[41–43] and can be fabricated using various inexpensive fabrication methods, such as colloidal self-assembly, hydrogels, and mold-based replica imprinting.[44–46]

In this review, recent incorporation of PC structures within emerging label-free biosensing platforms is discussed, including their applications for detecting proteins, nucleic acids, allergens, pathogens, and cancer biomarkers.[47–50] We will also provide a broad overview of PC structures and PC-based biosensors and their potential utilization as POC diagnostic tools. We describe various aspects of PC-based biosensors, including (i) PC structures and fabrication techniques, (ii) principles of PC-based biosensing, (iii) emerging technologies incorporating PC-based biosensors for potential POC applications, (iv) multi-target detection capability for PC-based biosensors, (v) surface chemistry approaches, (vi) current challenges and limitations for biosensors at the POC, and (vii) future outlook for PC-based biosensors at POC diagnostics.

2. Photonic crystal structures and fabrication techniques

PC structures consist of spatially arranged periodic dielectric materials that uniquely interact with light, providing high efficiency reflection at specific wavelengths. There are many examples of PC-type periodically nanostructured surfaces observed in nature.[51] For instance, the bright iridescent color of the *Morpho rhetenor* butterfly,[52] peacock,[53] *Eupholus magnificus* insect,[54] sea mouse[55] and opals[56] are all associated with the geometrical arrangement on their surface, where broadband light illuminates and reflects through PC structures (Fig. 2).[52] In practice, PC structures can be fabricated in one-dimensional (1-D), two-dimensional (2-D) or three-dimensional (3-D) orientations incorporating microcavities,[57] waveguides,[58] slabs,[59] multi-layered thin films,[60] and porous geometries[61] (Fig. 3). A diverse range of materials, such as silicon (Si),[62] glass,[63] polymers,[64] colloids,[65–68] and silk,[69–71] are used in the fabrication of PC structures (Table 1).

PC structures are fabricated using various methods, including self-assembly and lithography techniques. For instance, colloids composed of hydrogel polymers,[72] silica,[73] or polystyrene[74] are transferred from solution and self-assembled (*via* sedimentation, spin coating, or vertical deposition[44,75]) onto a surface to create PC structures that reflect iridescent color.[75–77] In addition, hydrogels are utilized in combination with colloidal particles in the fabrication of PC structures. While these self-assembly methods are inexpensive, precisely controlling the dimensions and geometry of the underlying PC structure is difficult. Top-down approaches, including electron beam lithography (e-beam), nanoimprint lithography (NIL), electrochemical etching, and thin film

Table 1 General overview of PC-based biosensors

Geometry of PC	Material used	Analyte detected	Limit of detection	Ref.
Hollow core waveguide	SiO_2	EGFR (cancer biomarker)	100 pg nL^{-1}	235
Hollow core waveguide	SiO_2	AFP (hepatocellular carcinoma biomarker)	NA	190
Hollow core waveguide	SiO_2	MCF-7 (breast cancer biomarker)	20 pg/50 nL	191
Microcavity coupled waveguide	SOI	ZEB1 (lung cancer cells)	0.67 ng mL^{-1}	189
Beam cavity	Si/SiO_2	CEA (colon cancer)	0.1 pg mL^{-1}	192
1-D slab	TiO_2/quartz	Various breast cancer biomarkers	4.1 pg mL^{-1}	193
Colloidal spheres	Si on glass	DNA–drug interaction (daunorubicin)	NA	99
Colloidal spheres	Polystyrene	DNA	13.5 fM	188
1-D slab	TiO_2/SiO_2	DNA-MaZEF (DNA binding protein)	NA	173
2-D waveguide holes	SOI	ssDNA	19.8 nM	98
Slotted 2-D holes	SOI	Avidin	1 μg mL^{-1}	124
Slotted 2-D holes	SOI	IgG, biotin proteins	0.1 pg mL^{-1}	237
Cavity with hole defects	SOI	BSA	20 pM	177
Microcavity slot	SOI	BSA	2.1 pg mm^{-2}	238
1-D slab	TiO_2/quartz	EGFR, uPAR	~pg mL^{-1}	227
Porous Si	Si	Pepsin enzyme	7.2 pmol	178
Porous Si	Si	Subtilisin protease enzyme	0.37 pM	103
Porous Si/hydrogel	Si	*E. coli* bacteria	10^3 cells per mL	239
2-D holes	Cyclo-olefin polymer	Influenza virus from saliva	1 ng mL^{-1}	93
2-D polymer pillars	Acrylate-based polymer	*L. pneumophila* bacteria	200 cells per mL	96
2-D holes with point defects	SOI	HPV virus-like particles	1.5 nM	92
1-D slab	TiO_2/polymer	Rotavirus	36 FFU	94
1-D slab	TiO_2/polymer	HIV-1	10^4 copies per mL	91
Porous Si	Si	*E. coli* bacteria	200 cells per mm^2	95
1-D slab with cavity layers	TiO_2/PMMA/Si	Anthrax DNA	0.1 nM	100
2-D holes with line defects	SOI	Human IL-10 antibody	20 pM	240
Colloidal spheres	Polystyrene	Avidin	100 ng mL^{-1}	123
Inverse opals	Silica	IgG protein	0.5 mg mL^{-1}	157
Colloidal spheres	Silica	Mycotoxins	0.5 pg mL^{-1}	196
2-D holes with point defects	SOI	BSA	2.5 fg	175
Colloidal spheres	Polystyrene/hydrogel	Glucose, fructose	250 μM	241
Colloidal spheres	Polystyrene/copolymer	Glucose in tear and blood	0.15 nM	105
Colloidal spheres	Ag in hydrogel	Glucose in urine	90 μM	41
Colloidal spheres	Ag in hydrogel	pH of urine	NA	201
2-D holes	SiN	Water, acetone, IPA	NA	242
1-D slab	TiO_2/amonil/glass	Streptavidin, CD40L antibody	24 ng mL^{-1}	136
Slotted 2-D holes	SOI	Avidin	15 nM	124
Slotted 2-D holes with defect	SOI	BSA	4 fg	35
Colloidal spheres	SiO_2 nanoparticles	Human IgG	~mg mL^{-1}	243
1-D slab	TiO_2/polymer	IgG protein	0.5 mg mL^{-1}	46
1-D slab	TiO_2/SiO_2	Human IgG	0.5 mg mL^{-1}	119

deposition techniques,[78,79] are alternatives to bottom-up self-assembly methods. Briefly, in the e-beam process, an electron beam is used to write a desired pattern onto a substrate (often silicon), which is previously coated with an electron-sensitive resist. The resist is then developed, and the electron-beam pattern is transferred to the substrate *via* etching. Performing this method requires e-beam lithography devices, which are large, expensive and require skilled operators. NIL is a rapid, simple, and scalable pattern transfer technique alternative to e-beam lithography.[80] In NIL, a pattern is initially produced using deep UV/e-beam lithography on a master mold, which can be easily transferred to daughter replicas. The NIL method has been used to mass-produce PC structures rapidly and reliably; however, only a finite number of replicas can be generated from a single mold due to wear.[79] Electrochemical etching can be used to fabricate porous Si structures that produce a photonic band gap due to formed periodic trenches. Electrochemical etching of Si is inexpensive and can be performed in research labs. Although trenches and channels provide a higher surface area for chemical interactions, large biomolecules may cause aggregation and blocking of the channels (*e.g.*, cells) when using clinical samples.

Overall, a wide range of materials and fabrication methods is available for the development of PC structures. Using PC structures for POC applications is highly feasible due to the availability of inexpensive fabrication materials such as hydrogels and colloidal particles and the scalable production method using NIL. The theoretical background behind the PC phenomenon and how these PC structures are used as biosensors are discussed in the following section.

3. Principles of PC-based biosensing

A periodic arrangement of dielectric materials creates a photonic band gap when a range of electromagnetic waves cannot propagate due to the destructive interference of incident light with reflections at dielectric boundaries.[81] PC structures can be produced from a variety of geometries, including Bragg reflectors, slabs, opals, microcavities, and colloids. An optical phenomenon describing most of these structures can be deduced from understanding a simple Bragg structure. A typical Bragg reflector consists of alternating high and low refractive index dielectric

Table 2 Comparison of PC-based biosensors with selected competing technologies

Parameters	Electrical sensors[115,216]	Plasmonic sensors[214]	Nanomechanical sensors[215]	Magneto-sensors[244]	Photonic crystal sensors[193,234]
Fabrication method	• Two rail electrodes are patterned on transparent substrates using silver ink. • There is no need for clean room facility.	• Fabricating these sensors requires surface sensitive techniques employed at clean room facility.	• The system utilizes specialized nanomechanical sensors (cantilevers), which are expensive, and are fabricated through clean room techniques.	• Producing these sensors requires multi-step fabrication techniques at clean room facility.	• Self-assembly of colloids (simple and inexpensive) e-beam/photolithography (requires clean room) and NIL (can be used for mass production).
Assay complexity	• They require some sample pre-processing steps to replace ionic content with non-ionic fluids. • In the process, they also need multiple washing steps.	• The assay requires filtration steps to concentrate the exosomes in the samples.	• The system requires powerful isolation components to avoid fluctuations in temperature and vibration.	• They require dual-labeling to increase signals, as well multiple washing steps.	• Sample pre-processing required. However, it can be integrated into microfluidics to allow on-chip processing.
Assay time	>2 hours	<1 hour	<1 hour	>2 hours	>2 hours
Multi-target detection	• Possible, the platform is validated with distinct viruses and bacteria.	• Possible. The platform is assessed for only exosome samples with different surface markers.	• Possible. The platform is validated with two different antibiotics (vancomycin and oritavancin).	• Possible. The system is evaluated with only various protein biomarkers.	• Possible. In particular, the readout system can be integrated with a bundle of fibers for simultaneous multidetection from a 384 well.
Read-out	• The system employs an impedance-based read-out.	• Spectral readings coupled with transmission mode.	• Require temperature and vibration isolators.	• The platform utilizes magnetic field-based measurements.	• Spectral reading coupled with reflected mode.
Clinical testing	• Possible. There are clinical validations with blood, serum, and saliva.	• Possible. There is a clinical validation study with ascites.	• Possible. The platform is validated by some spiked experiments in serum samples.	• Possible. There are clinical validations with serum, urine, and saliva.	• Possible. A number of clinical validations were performed using blood, urine, saliva, and serum.

thin film layers (Fig. 4a). The optical thicknesses of these layers are designed to be one quarter of the wavelength of incident light (λ) (eqn (1)). Multiple reflections from consecutive layers provide constructive interference and result in total reflection (Fig. 4b). Light at this reflected wavelength resides in a photonic band gap region (Fig. 4c), and cannot propagate at normal incidence.[82]

$$d_{\text{high}} n_{\text{high}} = d_{\text{Low}} n_{\text{Low}} = \frac{\lambda}{4} \quad (1)$$

Another common PC structure is comprised of periodically modulated thin films, which are known as 1-D slabs. 1D-PC structures are commonly fabricated from a high refractive index coating layer over a periodically arranged low refractive index grating layer (Fig. 4d). In these PC gratings, only the zeroth order mode is allowed, while higher order modes are restricted at normal incidence, provided that the period of the grating (Λ) is smaller than the wavelength of the incident light ($\Lambda < \lambda$). Gratings of this type are also called subwavelength gratings, and exhibit efficient optical resonances.[83] Subwavelength PC gratings can be designed to reflect a narrow band of wavelengths and produce a sharp peak in the reflection spectrum (Fig. 4e).[84,85] Resonance occurs when a diffracted mode from the grating couples to a leaky waveguide mode. Radiation from the leaky mode constructively interferes with the reflected wave and destructively interferes with the transmitted wave, resulting in a resonant reflection.[83] The resonance wavelength peak is determined by the period (Λ) of PC gratings and the effective refractive index (n_{eff}) under resonance conditions (eqn (2)).[86]

$$\lambda_{\text{resonance}} = n_{\text{eff}} \Lambda \quad (2)$$

This resonance behavior of PC gratings is highly sensitive to the localized changes in dielectric permittivity on the crystal surface, which makes it suitable for sensing applications. In this regard, PC structures are widely utilized to develop sensing platforms for multiple applications of chemical sensing, environmental sensing, and more specifically, biosensing.[87–90] Briefly, a biochemical interaction (*e.g.*, binding) on the PC surface causes a change in the effective refractive index, which results in a shift of the resonance wavelength peak, which is proportional to the concentration of the biotarget (Fig. 5). PC structures have gained significant attention as sensitive transducers and have been incorporated into biosensors that capture, detect, and quantify various biological molecules, such as pathogens,[7,47,91–96] DNA,[97–101] proteins, enzymes,[102,103] glucose,[42,104–106] cells,[107,108] toxins,[109] and allergens.[110]

4. Emerging technologies incorporating PC-based biosensors for potential POC applications

Recent advances in microfluidics, telemedicine, flexible materials, and wearable sensing technologies hold promise to provide compact and portable platforms in biosensing applications at POC for the rapid, reliable, accurate, on-site, and label-free detection of biotargets.[111–118]

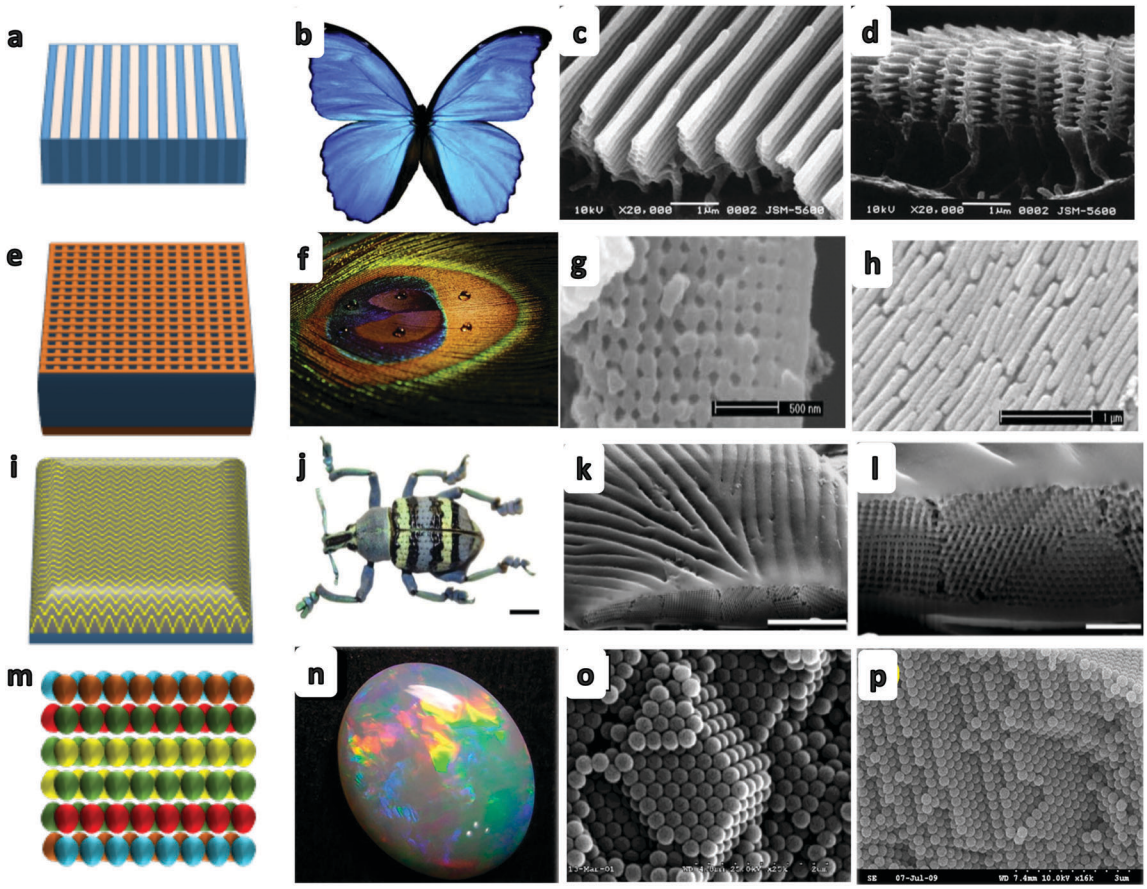

Fig. 2 PC structures commonly found in the nature. Bright iridescent color of these objects is due to the presence of geometrical periodic elements in their structures. Shown are four types of PC structures: 1. (a and b): 1-D (*Morpho rhetenor* butterfly), 2. (e and f): 2-D (peacocks);[53,225] 3. (i and j): 3-D (*Eupholus magnificus* insect); and 4. (m and n): colloidal (opals) structures.[56,226] The first column shows schematics highlighting the spatial arrangements of crystals within structures. The second column shows the actual picture of the example of the given PC type in the nature. The third and fourth columns show the SEM images of each example. Subfigures c and d were reproduced from ref. 52, with permission from Elsevier, copyright (2002), subfigures b and f were reproduced from ref. 225 with permission from Elsevier, copyright (2011), subfigures g and h were reproduced from ref. 53, copyright (2003), with permission from National Academy of Sciences, subfigures j, k, and l were reproduced from ref. 54 with permission, subfigure n was reproduced from ref. 228 with permission, subfigure o was reproduced from ref. 56 with permission, and subfigure p was reproduced with permission.

4.1 Microfluidics

Microfluidics technology offers considerable benefits to biosensing systems, particularly the POC devices. These advantages include (i) inexpensive fabrication materials (*e.g.*, glass, paper and polymers), (ii) ability to control low sample volume, (iii) ease of integration with optical platforms, and (iv) flexibility in producing multiple channels to allow multiplexed testing platforms.[119–121] PCs-integrated with microfluidic technologies are emerging as powerful biosensing diagnostic tools with the integration of these features.[50,122] For instance, integration of 1-D PC slabs within a microfluidic channel network at the bottom of a 96-well plate was used to detect immunoglobulin gamma (IgG).[46] This microfluidic-integrated platform enabled the concurrent multiplex detection of molecules using only 20 μL of the sample (Fig. 6). In another study using a colloidal polystyrene-based PC structure integrated with microfluidics, IgG molecules were captured and detected down to mg mL^{-1} levels.[123] PC structures have also been incorporated with polymer microfluidic channels to detect proteins; for example, a slotted PC cavity fabricated from Si was shown to detect 15 nM of avidin protein.[124,125]

4.2 Telemedicine

Smartphones have been increasingly utilized in medical diagnostics and healthcare applications, such as cell counting from whole blood, immunoassay testing, and imaging.[111,126,127] Smartphones will likely play an important role in the development of new biosensing platforms due to their wide availability, portability, compactness, capacity for data processing, ease of integration with microfluidic devices, and high-resolution optical components.[111,128] Recently, camera and optical systems in cellphones have been integrated with microfluidic, microscopy, and photonic crystal technologies for the spectral analyses of biosensing applications.[126,129–134] For instance, a 1-D PC slab was integrated with a smartphone to measure IgG concentration. The phone camera was used as a spectrometer to measure the transmission spectrum from the PC structures.[135] Although the system produced a reliable dose–response curve, adsorption of

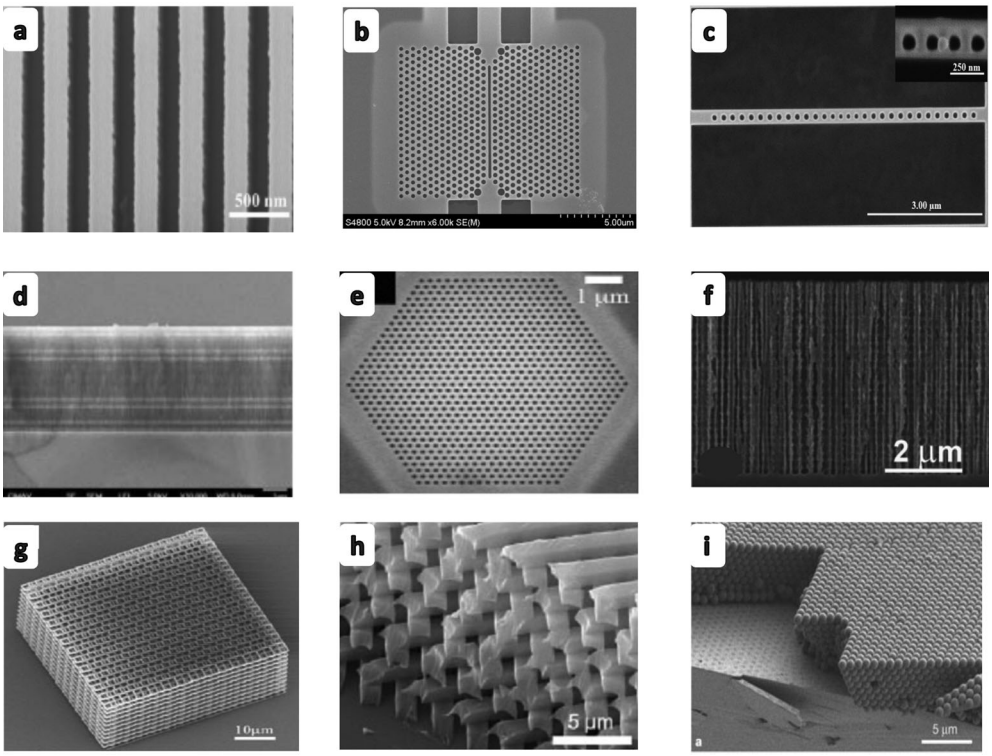

Fig. 3 Types of photonic crystals. (a) 1-D slab is one of the most exploited PC structures for biosensing applications. Refractive index alternates in one dimension only (in *x*, or in *y* axis) by forming air gaps in between substrate structures.[227] It also possess a refractive index contrast between coating layers as having high and low refractive indices (in the *z* axis). (b) 2-D holes with a line defect. Line defect creates a highly confined band gap region.[125] (c) Beam cavity. Periodic holes are fabricated on a column of a beam that is highly sensitive to refractive index changes.[228] (d) Bragg films. Multiple layers of thin films form a Bragg mirror, resulting in an approximately 100% reflection.[61] (e) 2-D holes. Refractive index alternates in two dimensions.[229] (f) Porous Si structures. Porous structures are fabricated using electrochemical etching on a Si substrate, which produces a band gap. Reproduced from ref. 230 with permission from The Royal Society of Chemistry. (g) 3-D PC structure. These highly periodic and fine features, where the periodicity of refractive index varies in all 3 dimensions, are fabricated using multiple consecutive e-beam steps under lab conditions. Reproduced from ref. 231 with permission from John Wiley and Sons. (h) Unique periodic 3-D PC structures. Reproduced from ref. 232 with permission from John Wiley and Sons. (i) Colloidal PCs. These PCs incorporate homogenous colloidal particles coated on a substrate. Reproduced from ref. 233 with permission from the Nature Publishing Group.

biomolecules could only be measured under dry conditions. Thus, further study with aqueous samples is required before this platform could be used to directly analyze clinical samples at the POC. In another study, a 1-D PC slab was integrated with a complementary metal–oxide–semiconductor (CMOS)-based smartphone camera to detect anti-recombinant human protein CD40 (Cluster of Differentiation-40), streptavidin, and anti-EGF antibody (Fig. 7).[136]

Smartphone-integrated platforms hold promise to address portability related issues at the POC, though their direct use in clinical applications is challenging because complex specimens, such as blood and tissue, need to be preprocessed before being brought into contact with the device.

4.3 Wearable and flexible sensors

Wearable sensors and flexible materials have recently gained attention for continuous and real-time monitoring of the physiological parameters and general health status of individuals.[137–142] For instance, they have been employed to measure the heart rate, skin temperature, blood oxygen levels, and more recently glucose sensing from sweat.[143–145] Wearable sensors are currently worn as wristbands, skin patches, and fabric patches. From a fabrication perspective, various nanotechnology-based techniques and materials are used for the production of these flexible and wearable sensors. In a recent study, a PC structure was designed with 2-D holes (with a diameter of ~100 nm) to evaluate strain changes.[146] This flexible sensor could be bent without losing its optical properties (Fig. 8a and b), and provided a sensitivity that was independent of deformation. In another study, colloidal polystyrene spheres were deposited on a flexible polyimide film.[147] A strain applied over this flexible film resulted in a blue shift in the reflection maxima (Fig. 8c and d).

3-D PC structures have also been incorporated into wearable sensors. For example, 3-D PC structures were investigated under pressure and may conceptually be used for detecting the severity of blast exposure to evaluate traumatic brain injury of soldiers in the battlefield.[148,149] In this study, 3-D voids were fabricated in an SU-8 resist to create 3-D PC structures that exhibited a color in the visible spectrum. These structures were exposed to varying high pressures (410 to 1090 kPa) to measure blast strength (Fig. 8e), and it was determined that large external forces could be detected by visual inspection (Fig. 8f–h). The PC structure

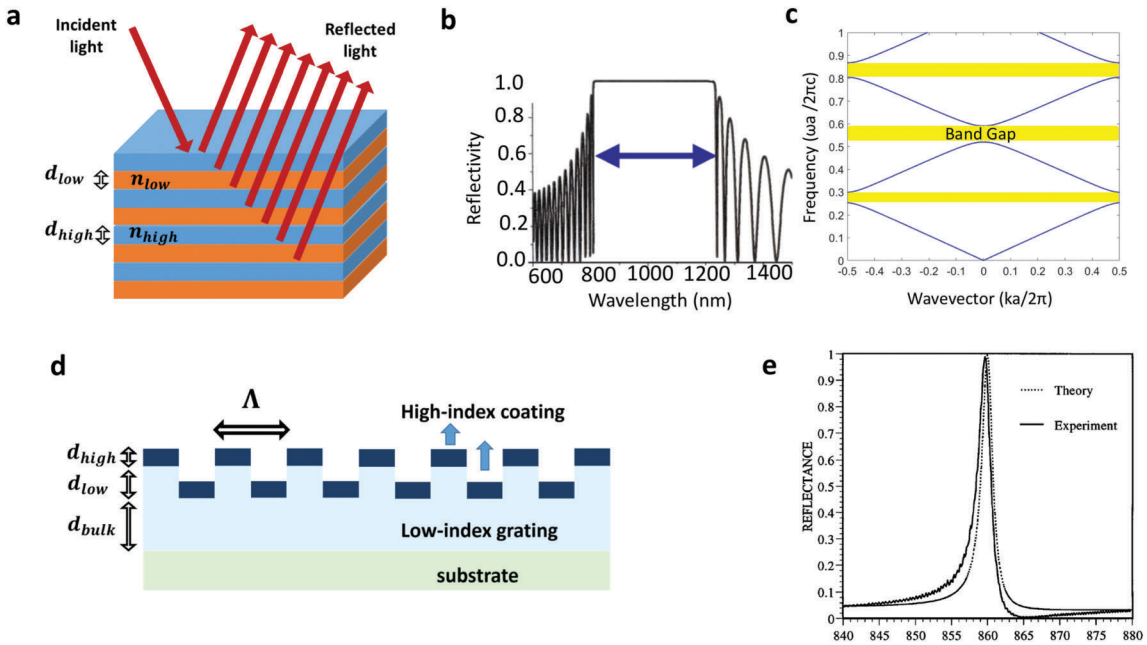

Fig. 4 The design and optical response of simple PCs. (a) A Bragg reflector consisting of alternating low and high refractive index of dielectric layers. At specific wavelengths, reflections from consecutive layers constructively interfere with each other and result in total reflection. (b) The reflection spectrum of a Bragg reflector.[82] The reflector has a photonic band gap region as shown by an arrow in near infrared wavelengths. Reproduced from ref. 82 with permission from IEEE, copyright (2002). (c) The photonic band structure of a 1-D PC. (d) The structure of a 1-D PC grating that consists of a low refractive index grating layer and a high refractive index coating layer. (e) Theoretical and experimental reflectance spectrum of a 1-D PC grating. The resonance reflection is observed at a wavelength of 860 nm. Reproduced with permission from ref. 84.

that was exposed to high external forces underwent structural deformation, resulting in a color change. This change was used to estimate the degree of pressure on the PC structure. While this work is promising, using these detectors on soldiers' uniforms is conceptual and their implementation in this field has not yet been evaluated.

4.4 Smart materials

Smart materials are an emerging class of responsive substances that can modify their physical or chemical properties, mostly reversibly, against external stimuli such as pH, temperature, electrical field, and light.[150,151] Smart materials, such as hydrogels, polyionic liquids, graphene, and carbon nanotubes (CNTs), have been used for various applications, including biosensing. In particular, their incorporation into PC structures holds promise for rapid, sensitive, and reliable biosensing. Hydrogel materials are 3-D nanostructured polymers consisting mostly of water. Hydrogels may be responsive to external stimuli, such as temperature, pH, or bio-stimuli such as antigen–antibody interactions.[45,72,152–155] For instance, PC structures comprised of hydrogel materials can be used as biosensors for the detection of DNA, proteins, antibodies and enzymes by monitoring the changes in lattice spacing or refractive indices.[41,43,156–159] In this respect, hydrogel-based PC structures provide either quantitative spectral results or qualitative naked-eye detection of biotarget concentrations.[41] Hydrogel-based PC structures hold great promise for POC applications owing to their cost-effective fabrication and simple optical detection systems. In a recent study, a hydrogel-based nanoporous PC structure was employed for label-free detection of rotavirus with concentrations ranging from 6.35 μg mL^{-1} to 1.27 mg mL^{-1} (Fig. 9a and b).[160] Polyionic liquids (PILs) are a class of polymeric materials containing repeating ionic monomeric units, which have recently been demonstrated for sensing applications.[161,162] In one such study, PIL was used to fabricate a 3-D macroporous PC structure, that exhibited Bragg reflection in the visible wavelength range, to detect a variety of ions.[163]

Hydrogels can also be used in combination with other materials including graphene or carbon nanotubes (CNTs) to produce PC structures. In one such study, graphene oxide was deposited on a silicon wafer and embedded into a hydrogel matrix to detect beta-glucan.[164] Graphene based-PC structures have also been investigated for enhanced sensitivity biosensing.[165] In addition, CNTs were incorporated into PC structures that provided a photonic band gap in the visible light spectrum.[166] Recently, CNT-based PC structures were investigated for optical applications.[167–169]

Smart materials have been studied extensively and have the potential to be utilized as biosensors due to the unique properties of each material. However, they require further validation using clinical matrices.

4.5 Metamaterials

Recently, PC structures based on metamaterials have been investigated for various applications, including imaging and biosensing.[169–172] For instance, a PC metamaterial with a 3-D woodpile geometry was proposed to excite plasmons with high spectral sensitivity.[170] The proposed structure was a silver-coated

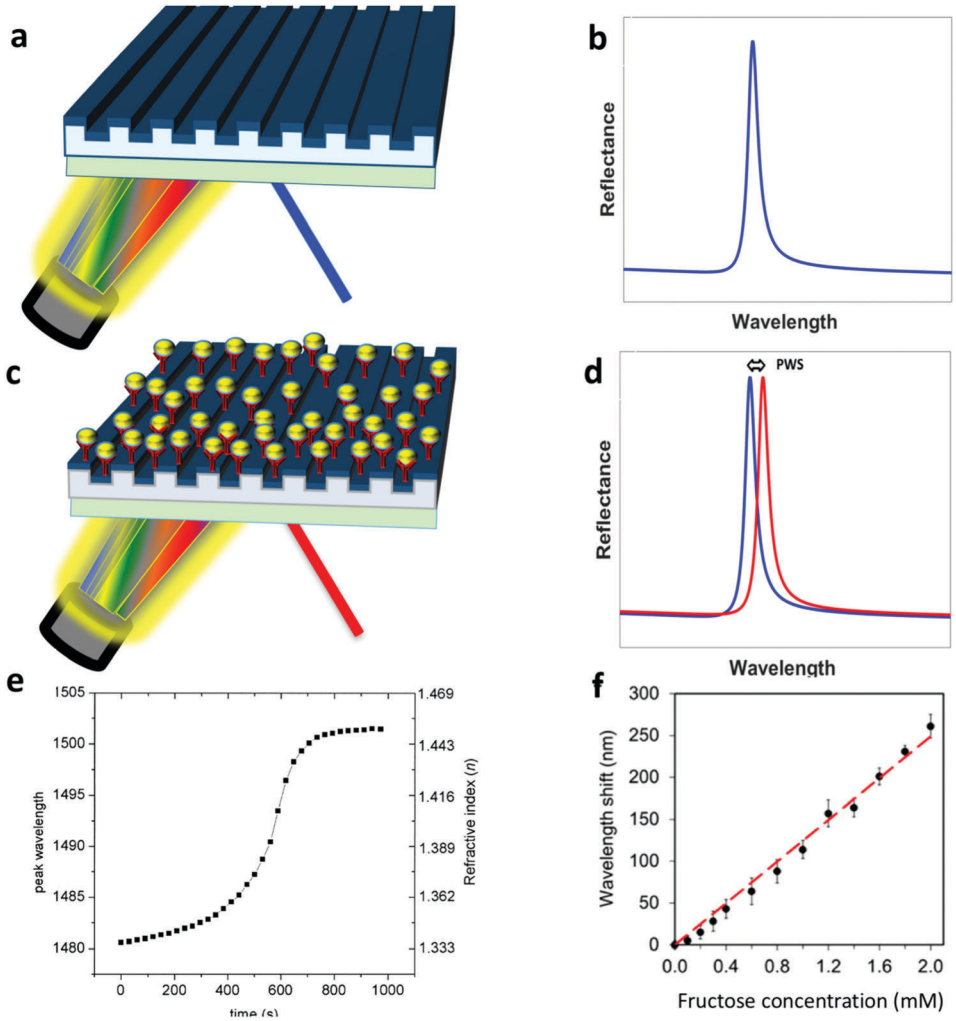

Fig. 5 Overall mechanism of biosensing using photonic crystals. (a) An example of the 1-D PC slab surface. (b) Corresponding resonance peak wavelength for this PC slab. (c) Functionalization of the slab surface and biological binding event *via* antigen–antibody interaction. (d) Peak wavelength shift (PWS) as a result of this interaction. (e) PWS corresponding to the refractive index change in a given time period.[236] (f) Dose–response curve in a biosensing event. Correlation between the concentration of the analyte and PWS.[41]

woodpile crystal providing a high surface-to-volume ratio with a sensitivity more than 2600 nm per refractive index unit (RIU) (Fig. 9c and d). In another study, a hyperbolic metamaterial biosensor consisting of 16 alternating layers of thin Al_2O_3 (aluminum oxide) and gold layers was demonstrated to detect biotin (Fig. 9e) with very high sensitivity up to 30 000 nm per RIU.[171] This 1-D multilayer structure supported guided modes ranging from visible to near infrared, enabled optical biosensing at different spectral regions with ultra-high spectral sensitivity, and detected 10 pM biotin in phosphate buffered saline (Fig. 9f). Light coupling was achieved with a 2-D gold diffraction grating on top of the multilayer films, eliminating the need for additional optical elements (*e.g.*, prism). Although metamaterial-based biosensors enable label-free detection with high sensitivity, they require multiple fabrication steps and may not be compatible with clinically relevant matrices (*i.e.*, whole blood, urine, and saliva).

Overall, the integration of PC structures with emerging technologies is promising for biosensing applications at POC owing to compact, flexible, and easy-to-use platforms. In particular, PC-based biosensors composed of smart materials may create a new class of flexible and wearable POC sensors with high sensitivity.

5. Multi-target detection capability for PC-based biosensors

PC-based biosensors have been employed to detect multiple biological targets, such as pathogens, proteins, nucleic acids, and glucose, for the diagnosis of a broad range of diseases, including diabetes and cancer. Here, we provide a broad perspective of using PC structures to quantify various molecular interactions ranging from biotin–streptavidin to cancer biomarkers.[173]

5.1 Protein detection

PC structures have been used to capture and detect numerous proteins, such as protein A, Immunoglobulin Gamma (IgG),

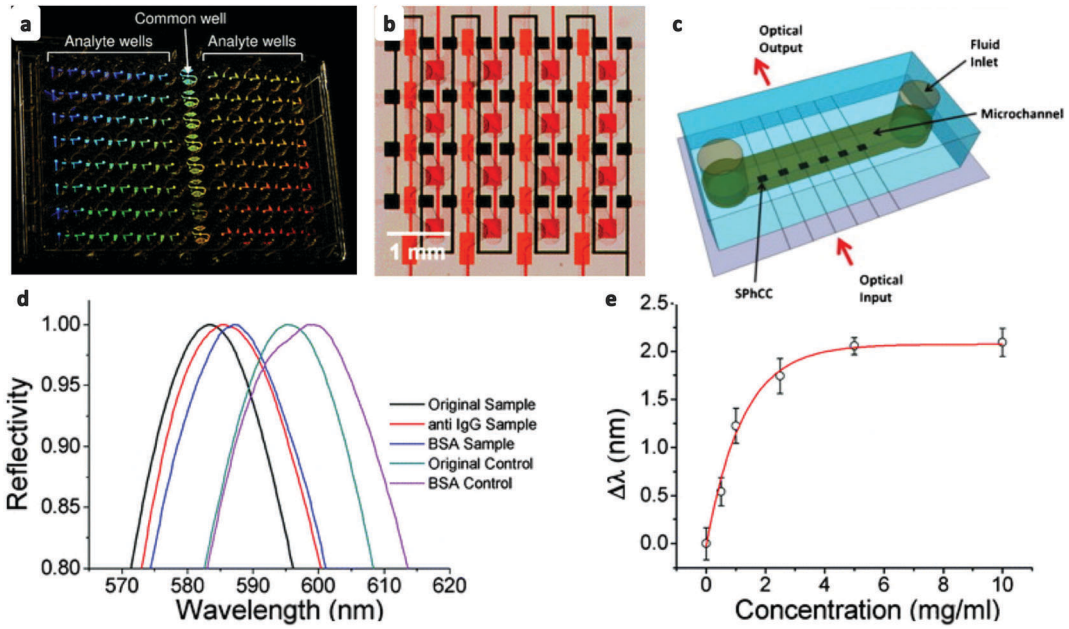

Fig. 6 PC biosensors integrated with microfluidic platforms for POC applications. (a) Multi-well plate integrated with a network of microfluidic channels with PC-based biosensors at the bottom. Reproduced from ref. 46 with permission from The Royal Society of Chemistry. A varying color difference was observed within the plate as the concentration of the analyte was changing. (b) A multi-valve microfluidic platform integrated with PCs for biosensing applications. Reproduced from ref. 119 with permission from The Royal Society of Chemistry. (c) Drawing of a microfluidic channel integrated with multiple PC (black rectangles) for optofluidic biosensing applications. Reproduced from ref. 124 with permission from Elsevier, copyright (2011). (d) PWS graph on a PC integrated with microfluidic channel. (e) PWS values as against an increasing concentration of IgG protein in the same microfluidic channel. Reproduced from ref. 243 with permission from The Royal Society of Chemistry.

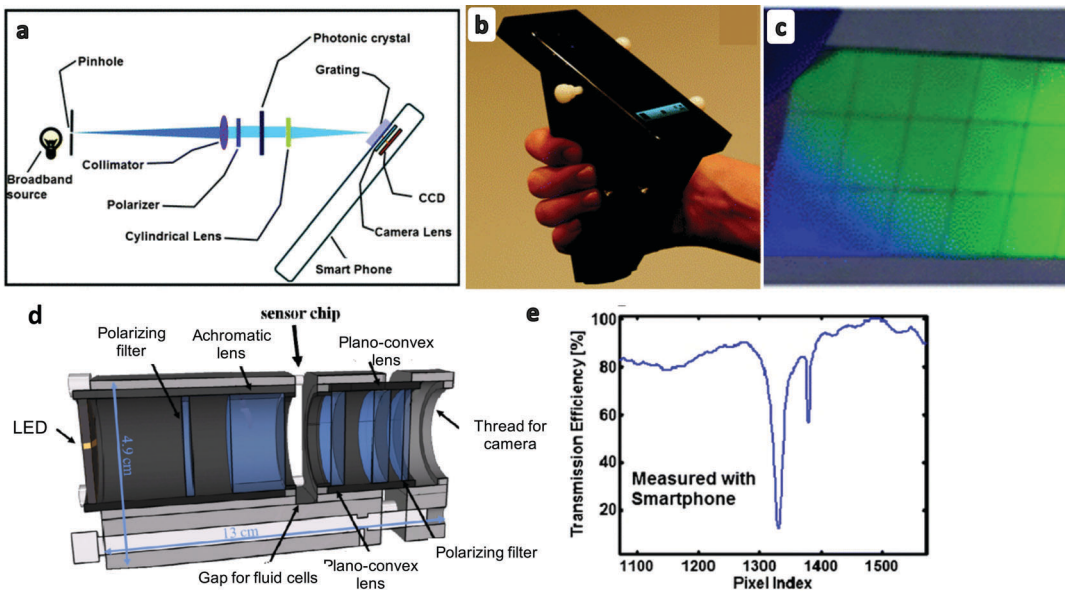

Fig. 7 PC structure integrated with a smartphone for biosensing applications at the POC. (a) Drawing representing a general scheme of a PC incorporated smartphone. The CCD camera of the phone was utilized as an optical sensing element. (b) Actual image of the PC smartphone platform. (c) The PC cartridge fits in a cradle to facilitate the light interaction with PC surfaces. (d) Drawing of another smartphone that employs a PC biosensor. An LED light source was collimated and directed to the PC surface and the transmitted light was captured by the smartphone camera. Reproduced with permission from ref. 136. (e) The spectrum of the PC surface measured with a smartphone CCD camera. Subfigures a, b, c, and e were reproduced from ref. 135 with permission from The Royal Society of Chemistry.

bovine serum albumin (BSA), and Protein G.[157,174,175] Streptavidin is often used in conjugation with biotin in experiments to validate the sensitivity and detection limit of new PC geometries due to the extraordinary affinity of streptavidin for biotin.[123,176,177] PC structures have been employed to investigate the substrate specificity and catalytic activity of certain enzymes, such as

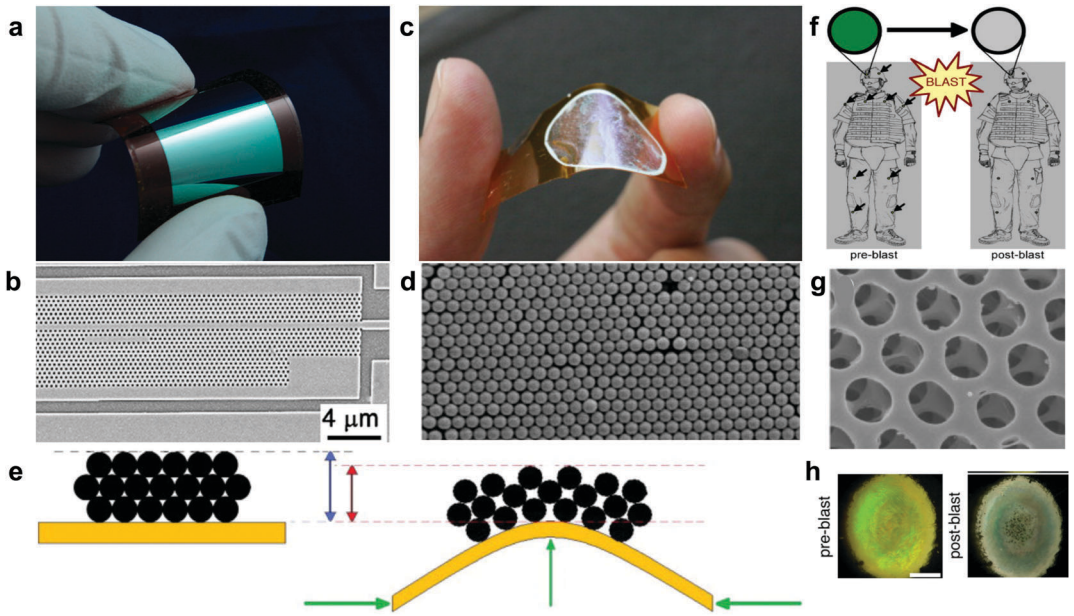

Fig. 8 Flexible and wearable PCs in sensing applications. (a) Picture of the Si membrane integrated with a photonic crystal. (b) 2-D holes with a waveguide to couple light into a flexible photonic crystal structure. Reproduced from ref. 146, copyright (2014) with permission from the American Chemical Society. (c) Flexible colloidal-based photonic crystals inkjet printed on a polyimide tape material under bending stress. (d) SEM image of the colloidal particles. (e) Schematic of the rearrangement of the colloidal particles against external pressure (bending). Reproduced from ref. 147 with permission from Elsevier, copyright (2016). (f) Possible use of PC structures as a blast sensor. In this concept, PC sensors could be worn on the soldier uniforms. (g) SEM image of the 3-D fabricated PC voids. (h) Image of the PC sensor before and after the blast. Reproduced from ref. 148 with permission from Elsevier, copyright (2011).

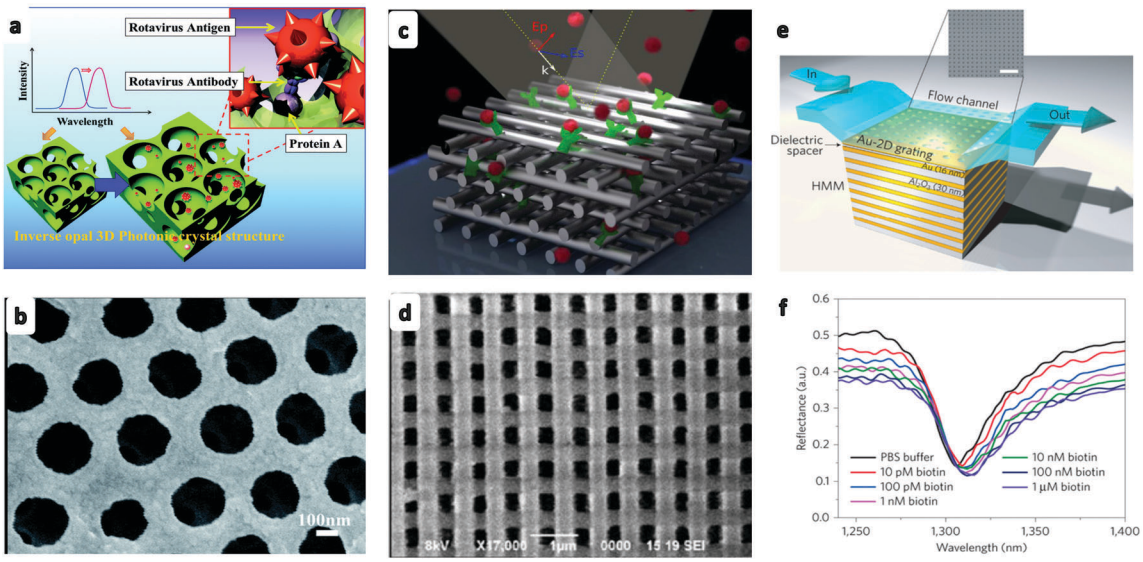

Fig. 9 Smart material- and metamaterial-based PCs for sensing. (a) Hydrogel-based PCs for the detection of rotavirus. (b) SEM image of the hydrogel structure. (a and b are reproduced from ref. 160 with permission from The Royal Society of Chemistry) (c) 3-D woodpile metamaterial-based PC structure coated with silver for sensing. (d) SEM image of the woodpile structure. (c and d are reproduced from ref. 170 with permission) (e) Multilayered thin film metamaterial integrated with gold grating for sensing applications. (f) Experimental wavelength shifts after incubation with varying biotin concentrations (e and f are reproduced with permission from Macmillan Publishers Ltd: [Nature Materials] (ref. 171)).

acetyl cholinesterase, pepsin and other proteases.[103,178] In one study, a porous Si-based PC structure was developed to evaluate proteolytic activities of pepsin and subtilisin proteases down to 7 pmol and 0.37 pM, respectively. When coupled with a fluorescence assay, a PC surface can significantly amplify the fluorophore intensity, increase the signal-to-noise ratio and reduce the detection limits. For example, a PC structure was coupled with fluorescence-labeled secondary antibody to detect

TNF-α concentrations at pg mL^{-1} levels.[185] The ability of an assay to detect disease targets at low concentrations at an early stage is very important. In this research, imaging of the PC spots was performed for the multiplex detection of different proteins.

Colloidal PC structures have also been widely employed for protein detection. For instance, arranged colloidal nanoparticles embedded inside a hydrogel were used to visually monitor a reflectance shift in response to protein concentration.[157] In this study, silica nanoparticles were embedded within a poly(ethylene glycol)-diacrylate hydrogel to generate a PC structure. This system was able to observe IgG proteins bound to protein A on the surfaces of the embedded nanoparticles. A color change from orange to green was observed after exposure to 10 mg mL^{-1} IgG, and the detection limit in the color shift was at the concentration of 0.5 mg mL^{-1} IgG (Fig. 10). Since this procedure uses a self-assembly deposition method and does not require advanced manufacturing technology, it is cost-effective; however, the concentrations necessary to observe a visual change are high, and thus, may not be compatible with sensitive detection applications.

By coupling with fluorescence-labeled secondary antibodies, PC-based biosensors have also been utilized to capture allergen-specific immunoglobulin (IgE) antibodies.[110,179,180] PC structures can enhance fluorescence signals when the optical resonance of the PC surface overlaps with either the excitation or emission spectra of a fluorophore. This enhanced excitation and emission yielded ~7500-fold increase in fluorescence signals.[181] In a recent study, a PC-enhanced fluorescence (PCEF) microarray platform was used to detect low concentrations of IgE in human sera with a limit of detection of 0.02 kU L^{-1}, which was comparable to current blood-based IgE detection methods.[110] However, current PC-based allergen platforms rely on fluorescence detection, which limits their use at the POC due to the requirements for labeling, additional instrumentation, and multiple assay preparation steps.

5.2 Nucleic acid detection

Biosensing of DNA, RNA, and DNA–protein interactions using PC-based platforms has been studied for various applications, including the determination of infectious agents, identification of genetic disorders,[182–185] and monitoring of DNA–protein interactions.[97,173,186] For instance, DNA and protein interactions were evaluated using a 1-D PC slab structure with a TiO_2 layer over a low index material, and DNA was detected down to nanomolar concentrations.[173] In this study, a panel of 1000 compounds were screened on a microplate-integrated PC-based biosensing platform (Fig. 11a–c). This platform uses multiple fibers, a motorized stage, and a coupled readout system (SRU Biosystems Bind Reader) capable of recording simultaneous readings from 384-wells. This platform has significant potential for drug-screening studies at the POC in resource-constrained settings since it incorporates a disposable and inexpensive 384-well microplate. The platform can further be utilized for the detection of RNA–protein and protein–protein interactions, and may shed light on gene expression at the cellular and molecular levels.[187] In addition to 1-D PC slab structures, colloid PCs have also been utilized for nucleic acid detection. In this study, self-assembled polystyrene beads were utilized to fabricate a colloidal PC structure that could detect

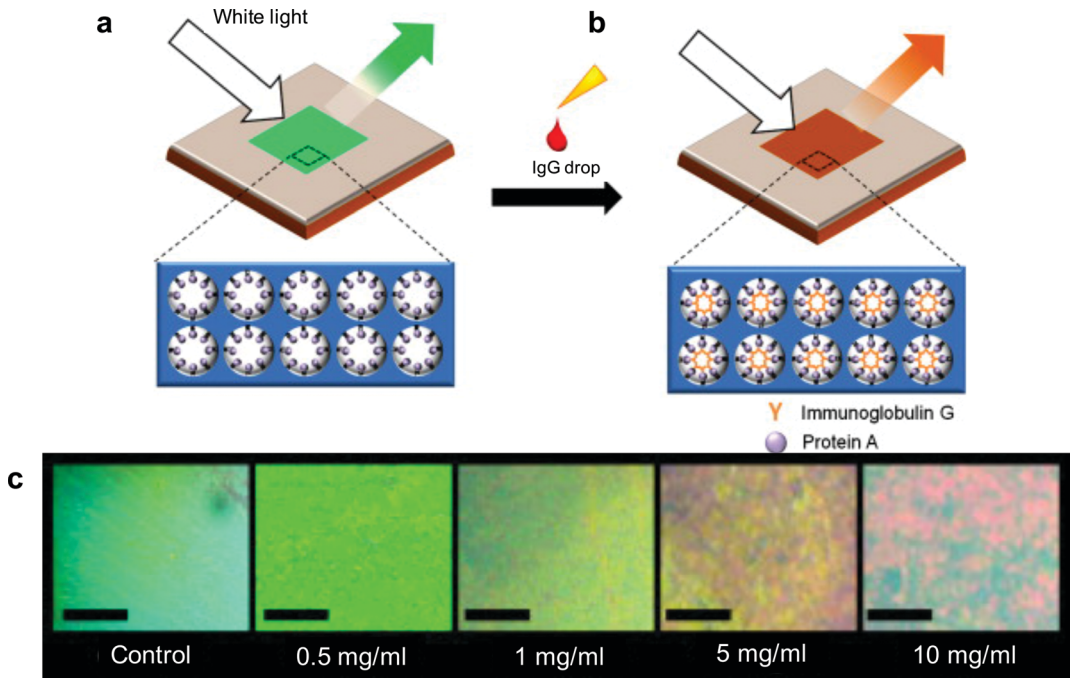

Fig. 10 PC biosensor for capturing and quantification of protein molecules. (a) Colloid PC structure was used to capture IgG proteins. (b) IgG bound to the colloid PC surface and changed the reflected color. (c) Image of the PC surface. A color shift was observed with the naked-eye as the concentration of IgG changed from 0.5 mg mL^{-1} to 10 mg mL^{-1} and the color of the sensor was transformed from green to reddish. Reproduced from ref. 157 with permission from Elsevier, copyright (2013).

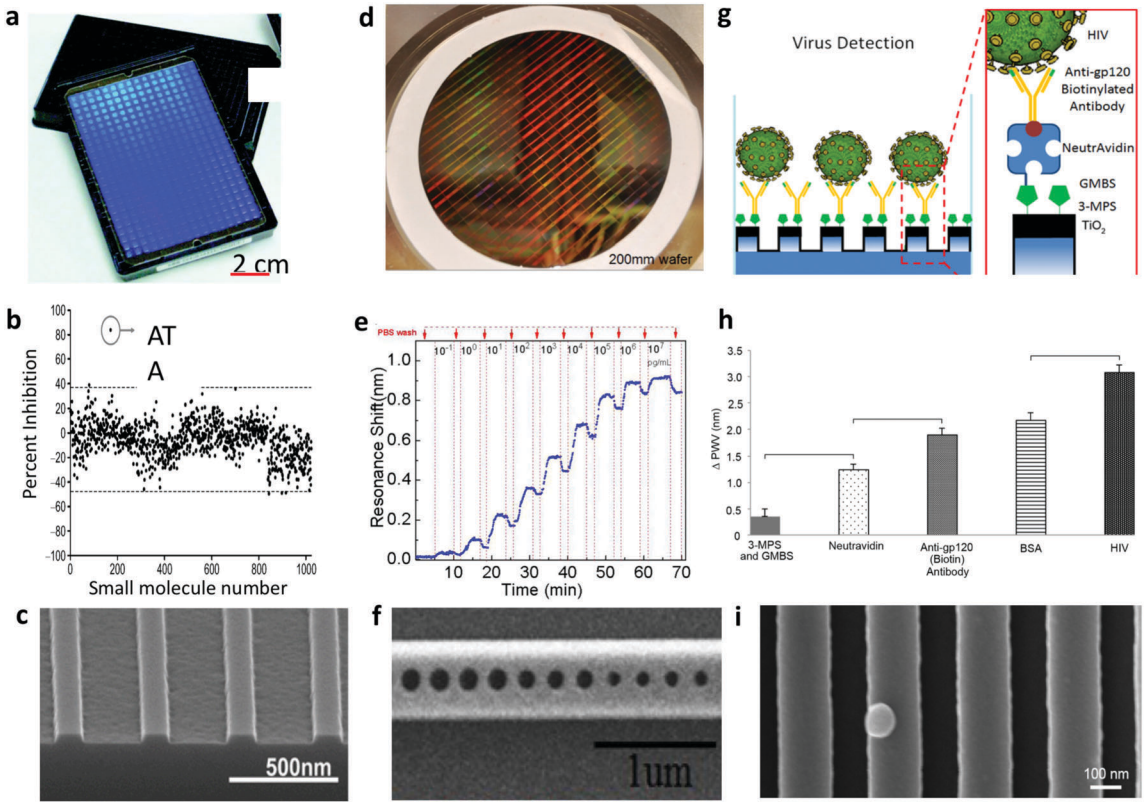

Fig. 11 Monitoring DNA–protein interaction using a PC biosensor. (a) Image of a 384-well plate integrated with a PC platform for drug screening. (b) Drug screening for protein–DNA binding inhibition. An outstanding molecule was recorded using a PC PWS. (Aurintricarboxylic acid, ATA molecule.) Reproduced from ref. 173 with permission, copyright (2008), from the American Chemical Society. (c) SEM image of the 1-D PC slabs used for drug screening. Reproduced from ref. 234 with permission from The Royal Society of Chemistry. (d) Image of a PC structure patterned on to an 8″ wafer (200 mm). (e) Resonance shift spectrum of PC on wafer over time, which was used to capture anti-CEA antigen for cancer detection. (f) SEM image of 1-D holes on a beam PC. Reproduced from ref. 192 with permission from The Royal Society of Chemistry. (g) Functionalization of 1-D PC slab surfaces with the antibody that is specific to virus surface antigens for capturing HIV.[91] (h) Peak wavelength shifts on the virus capturing after every step of surface functionalization. (i) SEM image of captured HIV on the PC surface. Reproduced from ref. 91 with permission from Macmillian Publishers Ltd: [Scientific Reports], copyright (2014).

hybridized DNA down to 13.5 fM.[188] In another study, a planar waveguide was employed for the detection of single-stranded DNA at a concentration of 19.8 nM.[98] The use of PC structures is a promising alternative to the conventional polymerase chain reaction (PCR) techniques for nucleic acid detection due to their low cost, ease-of-use, rapid response, and high detection capacities.

5.3 Applications in cancer

Biosensors are widely employed in the detection of biomarkers for diagnosis and prognosis of cancer. Currently, various biomarkers, such as epidermal growth factor receptor (EGFR), human epidermal growth factor receptor 2 (HER2), prostate-specific antigen (PSA), carcinoembryonic antigen (CEA), tumor necrosis factor-α (TNF-α), and calreticulin (CRT), are under clinical study for diagnosis of cancer.[189–191] Detecting these biomarkers at an early stage of malignancy can contribute to better treatment outcomes and significantly increase the quality of life for cancer patients.

Recently, PC-based biosensors have been employed in diagnosis and early detection of cancer.[189,192,193] In one study, a waveguide integrated with a cavity was employed for the detection of CEA protein for the diagnosis of colon cancer (Fig. 11d–f).[192] This platform provided a detection limit for CEA protein down to the 0.1 pg mL^{-1} level. In another study, a cavity and a line defect were fabricated on the surface of a silicon substrate to capture lung cancer cells.[189] In another study, 1-D PC slabs obtained from quartz materials were fabricated *via* NIL. This PC-based platform was used to detect 21 different cancer biomarkers, including HER2, EGFR, and prostate-specific antigen (PSA) with a detection range from 2.1 pg mL^{-1} to 41 pg mL^{-1}.[193] This multiplexed cancer biomarker platform can function in both fluorescence and non-fluorescence modes, providing flexibility to work with labelled and non-labelled biotarget sensing.

5.4 Pathogen detection

Rapid identification and quantification of pathogens, such as bacteria and viruses, is important for diagnosis and prognosis in the POC environments at resource-constrained settings. Recently, PC structures have been deployed at the POC for diagnoses of infectious diseases caused by pathogenic agents and toxins.[92,109,194] For instance, 2-D PC pillars, fabricated on polymer substrates

using NIL, were used for the detection of human influenza virus (H1N1) in human saliva. This platform can detect H1N1 antigens at a concentration as low as 1 ng mL^{-1}.[93] In another study, polymer-2-D pillar PC structures were used to detect *L. pneumophila* bacteria down to 200 cells per mL.[96] PC-based platforms can also be used for the detection of viruses such as rotavirus, HIV-1, and human papilloma virus-like particles.[92,94,195] To detect HIV-1, a PC surface was functionalized with anti-gp120 antibody for capturing HIV-1 ranging from 10^4 copies per mL to 10^8 copies per mL (Fig. 11g–i). In another study, silica microspheres were used to fabricate colloidal PC structures for the detection of multiple mycotoxins in cereal samples.[201] Although microspheres are fabricated inexpensively as droplets in water–oil two-phase flow, this system still depends on fluorescence measurements and may be subject to undesirable background variation due to the inherent labelling procedure.[196]

5.5 Glucose sensing

Detection of glucose holds significant importance in POC diagnostics for diabetics.[197,198] Although glucose sensors are globally available as POC tools, there is still a need for non-invasive glucose biosensing using new and advanced technology sensing platforms, including PC-based biosensors.[199,200] Non-invasive monitoring can be achieved by collecting samples other than blood such as sweat, tear fluid, and urine. For instance, a hybrid photonic structure (1-D Bragg gratings) was fabricated from silver nanoparticles and a hydrogel to detect glucose, fructose, and lactate. This platform was tested with urine samples from diabetes patients with a detection limit of 90 μM.[41] In another study, the poly(hydroxyethyl methacrylate)-based (pHEMA) matrix was UV cross-linked, and silver nanoparticles were dispersed in this hydrogel. A pulse laser was then used to align the silver particles in confined regions creating a periodic structure, which ultimately provided PC properties.[201] Furthermore, the platform was also tested in artificial tear fluid for accurate glucose sensing (Fig. 12). This platform is unique because it employs inexpensive hydrogels and can be linked to biomolecules by easy conjugation with carboxylic groups. In this study, PC structures were fabricated from polystyrene colloidal spheres integrated with hydrogel for glucose sensing at 50 μM.

Overall, although PC-based platforms have been employed for the detection of glucose with encouraging results, their widespread utilization for glucose sensing and diabetes diagnosis needs to be evaluated for reliable and accurate sensing.

6. Surface chemistry approaches in PC-based biosensing applications

PC-based biosensing platforms consist of an optically active layer and immobilized binder molecules, such as affibodies, nanobodies, peptides, antibodies, and antibody fragments to ensure biotarget capture.[157,158,202] Depending on the material type used for the optically active layer, binder molecules can be immobilized using various functionalization strategies, including physical adsorption (physisorption), covalent binding, and affinity-assisted coupling. Furthermore, anti-fouling agents play

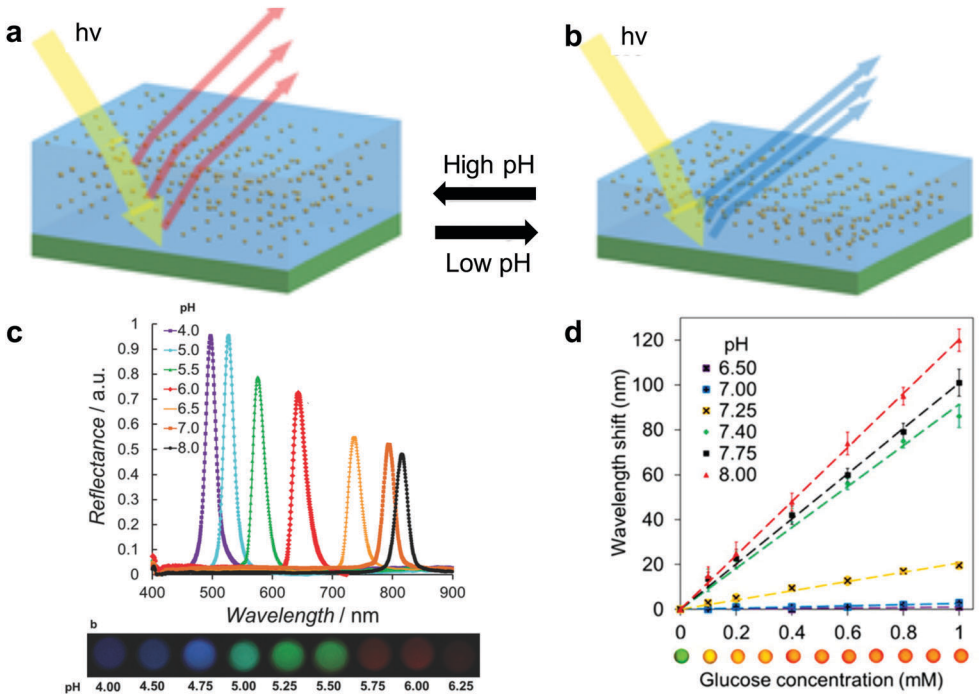

Fig. 12 Glucose sensing from urine using a PC biosensor. (a) Scheme of Ag incorporated hydrogel PC structure. (b) Simulation of a PWS as a result of the pH change. (c) The PWS at varying pH values and its corresponding observable color code. Reproduced from ref. 201 with permission from John Wiley and Sons. (d) Glucose concentration as a function of changing PWS at various pH and the color code of this shift.[41]

an important role in reducing the non-specific interactions and improving the sensitivity and specificity. In this section, we discuss surface chemistry approaches for TiO_2-, Si-, and SiO_2-based PC sensors, as well as anti-fouling agents to minimize non-specific binding.

Physical adsorption strategies are used to accumulate biotargets onto optically active layers *via* hydrogen bonds and van der Waals interactions. By applying plasma techniques, the net charge on a surface can be changed to increase the surface coverage of a biotarget.[203] For instance, PC waveguide structures with a Si layer were employed to monitor the physisorption of bovine serum albumin (BSA).[35] In this study, a BSA solution was directly applied to the PC waveguide surface and non-specific physical adsorption of BSA molecules was monitored. Although physisorption is simple, easy-to-apply, and does not require any wet-chemistry or laborious modification steps, it can interfere with other biomolecules in the detection buffer. Furthermore, physisorption is based on weak interactions between the surface and the biotarget, and is therefore not stable and can easily detach when surface charge is altered by changes in pH, ionic content, and temperature.

Covalent binding is one of the standard methods for immobilization approaches using the strong chemical linkage that forms between a sensor surface and binder molecules. TiO_2 and SiO_2 surfaces are common substrates for optical sensors; however, performing coupling on these surfaces is laborious since it requires layer-by-layer surface functionalization including surface activation, functional group generation, and binder immobilization. Silane-based molecules with a variety of functional groups are commonly used to immobilize biomolecules onto glass surfaces. A standard protocol for silanizing a surface begins with cleaning the surface using a strong oxidizing agent, such as piranha solution (a mixture of H_2O_2 and H_2SO_4) to increase the density of silanol groups exposed on a surface, which also increases the hydrophilicity of the sensor surface. Then, a silanization agent, such as (3-aminopropyl)triethoxysilane (APTES) or (3-aminopropyl)trimethoxysilane–tetramethoxysilane (MPTMS or 3-MPS), is applied to generate a self-assembled monolayer (SAM), which consists of hydroxyl groups, alkyl backbone chains, and functional tail groups.[204,205] Alkyl chains enable the height of captured biotargets to be adjusted from the sensor surface, and can also contain active tail groups, such as amine, carboxyl, and succinimide esters to tether binder molecules (Fig. 13).

The latter surface functionalization approach provides affinity-based interactions at specific regions on binders and anchor molecules.[206] However, clinical samples have a complex composition including proteins, lipids, and sugar units that can non-specifically adhere to a sensor surface. Non-specific binding can occur at active, passivated, and untreated areas on the sensor. Anti-fouling agents, including chemical modifiers, proteins, and polymeric substances, serve to prevent non-specific binding and increase the detection accuracy of target molecules. Furthermore, working with biospecimens requires sample preparation steps to avoid signal fluctuations and inaccuracies, considerably increasing the complexity of biosensing assays.[207,208]

7. Current challenges and limitations for biosensors at the POC

In this section, we discuss a number of emerging technologies with respect to challenges associated with current biosensors at the POC. These criteria include label-free sensing, assay complexity, assay time, multi-target detection, read-out mechanisms, fabrication methods, and applicability for clinical testing. We compare PC-based biosensing platforms with up-to-date biosensing technologies: nanomechanical sensors, plasmonics tools, electrical sensing platforms, and magnetosensors (Table 2).

7.1 Label-free biosensing

Labeling of biotargets, often with fluorescence molecules, has been extensively utilized in biosensing applications to enhance signal readout for improving measurements. However, introducing a label potentially adds complexity, increases experimental errors, and presents additional inefficiencies and uncertainties, such as quenching effects and photobleaching.[209] Additionally, labeling a biomolecule can significantly alter its characteristic properties (conformation, solubility, and affinity).[210] Considering the challenges associated with labeling, label-free assays can reduce cost, complexity, and time for POC tests by eliminating the use of labels, dyes, and high-volume of reagents.[211–213] Therefore, there is a demand for label-free, rapid, sensitive and accurate biosensing platforms at the POC, which will address the challenges associated with current label-based biosensor strategies. In this regard, PC structures represent a new class of biosensors that hold promise for label-free biosensing with potential applications at the POC.

7.2 Assay time

To be sustainable, emerging technologies need to provide rapid, inexpensive, and multiplexed solutions over existing assays and methods. Some platforms require filtration-type sample preparation steps to concentrate targets in the sample, which also increases assay complexity and time.[214] From a POC perspective, biosensing platforms need to be fabricated with inexpensive materials and methods using simple and inexpensive production techniques. For instance, some of the biosensing platforms require clean room facilities and multiple chemical etches for their fabrication, which may significantly increase the total assay cost.[214]

The read-out mechanism is another pivotal criterion to obtain reliable measurements at the POC. For instance, nanomechanical platforms, including quartz crystal microbalance and piezoelectric sensors, are affected by multiple external parameters such as temperature and vibration and require additional equipment (*e.g.*, vibration insulation and temperature control systems) to minimize these external interferences to ensure reliable measurements.[215] This additional equipment limits the portability and may also increase the cost, thus not satisfying some of the key requirements for a POC device.

7.3 Multiplexing capability

An ideal biosensing platform needs to detect multiple targets. This feature will provide a wide window to evaluate different

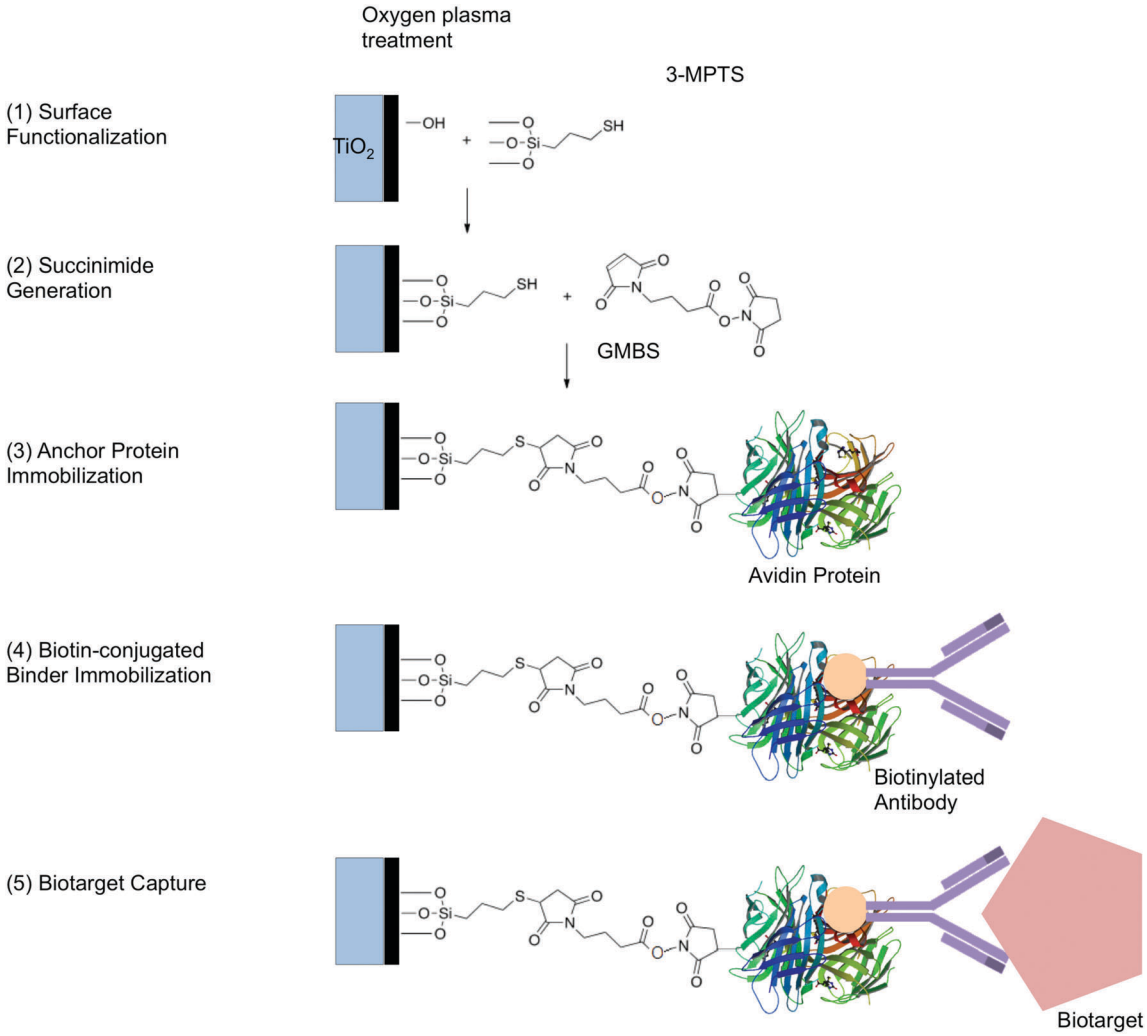

Fig. 13 Surface chemistry approaches for PC-based biosensors. Initially, the PC surface (*i.e.*, TiO_2) is treated with piranha solution and/or oxygen plasma to increase the hydrophilicity by exposing polar molecules on the surface. The surface is then immersed in a silane solution (such as 3-mercaptopropyltrimethoxysilane (3-MPTS)). The other end of bound silane is conjugated to a linker molecule (4-maleimidobutyric acid *N*-hydroxysuccinimide ester (GMBS)) containing a succinimide end-group. An anchor protein such as neutravidin can be immobilized using a GMBS linker molecule. A biotin-conjugated antibody can interact with neutravidin and then specifically bind to a desired biotarget molecule.

targets on a single platform, increasing its applicability for versatile POC testing. To immobilize various antibodies/binders onto a single sensor surface, PC-based biosensor platforms can benefit from antibody printing technologies (Table 2).[193]

7.4 Clinical validation

Biological specimens, such as blood, saliva, urine, and sweat, have distinct characteristics. These matrices have various ionic content, ionic strength, pH, and a diverse makeup comprised of cells, proteins, and lipids. Detecting biotargets in biological matrices constitutes one of the major challenges for biosensing. For instance, electrical-based sensing platforms measure electrical potential *via* different modalities, such as amperometry, potentiometry, and capacitance read-outs. Most of these platforms require replacing the biological matrix with non-ionic fluids, and therefore multi-step flow or centrifugation is required to minimize or eliminate interfering factors for read-out.[115,216] Ultimately, biosensors need to undergo extensive clinical validation before they can be used at the POC.

8. Future outlook for PC-based biosensors at POC diagnostics

The global biosensor market is valued at approximately US$ 13 billion in 2013 and projected to grow substantially to US$ 22 billion by 2020.[217] On-site (bedside) biosensors at the POC are poised to transform the healthcare industry as invaluable tools for the diagnosis and monitoring of diseases, infections, and pandemics worldwide. Advances in flexible, wearable, and implantable sensing technologies integrated with responsive materials can potentially connect patients to the clinic, thus providing continuous monitoring, such as glucose sensing for the patients with diabetes at the point-of-need.[218,219] Due to their

characteristics including flexibility (*e.g.*, hydrogels) and integration capability with smart materials (*e.g.*, CNTs and graphene), PC-based sensors will be an asset to the current wearable continuous monitoring tools and sensors.

A color shift that can be observed with the naked eye or with the help of a color legend is valuable at the POC. One interesting potential application for PC-based structures is to dynamically change the optical properties in response to environmental parameters, such as geometry, pH, and temperature. An example can be found in nature as suggested by a recent study on chameleon skin, which revealed the presence of guanine pillar-like nanocrystal PC structures.[220] When relaxed, crystals were randomly distributed, but changed to a square or hexagonally-packed lattice geometry when excited, thereby changing the skin's visible colors (Fig. 14). Inspired by this example, PC structures could also be fabricated as simple diagnostic tools to produce a color shift against an external stimulus with a subsequent change in geometry. This method may potentially eliminate the need for large and expensive optical devices for biosensors in the POC applications.

PC structures with more complicated geometries, such as 2-D PCs, are sensitive to changes in the refractive index in nano- and micro-scale volumes. Large wavelength shifts were experimentally observed after binding single sub-micron sized metallic and polymeric nanoparticles.[122,221–224] Detection of virus particles using these structures are highly promising, since viruses strongly interact with light, and can be easily captured on top of or inside photonic crystals.[34,194] However, biological detection of viral particles using 2-D PC structures has been difficult due to the low refractive index contrast between water and biological targets. Recent work with human papillomavirus-like particles spiked into serum has suggested that the detection of biologically relevant particles is possible, with a detection limit in the nanomolar range.[92]

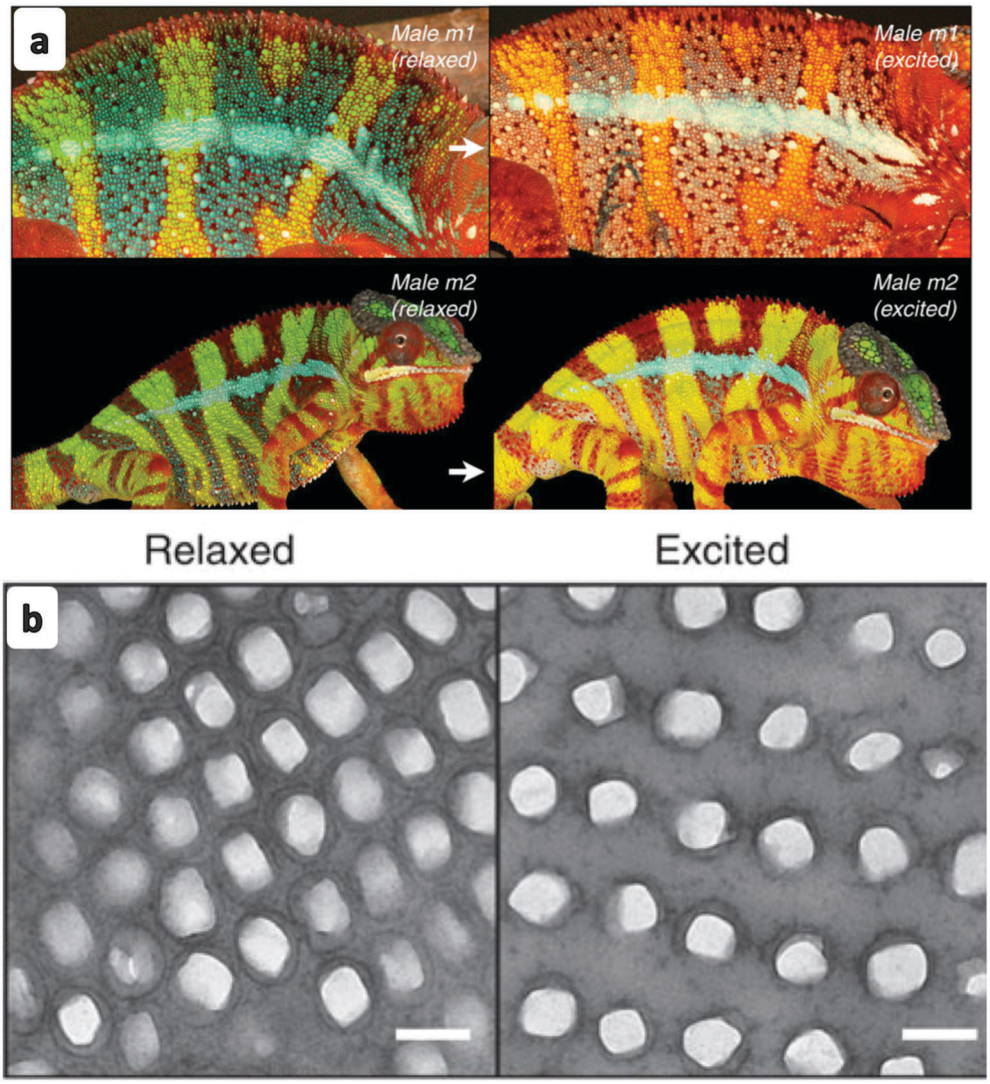

Fig. 14 Spatial arrangements of PC structures in chameleon's body. (a) The color change of two male chameleons. The left column indicates the relaxed state; the right column indicates the excited state. (b) TEM images of these two states. In the relaxed state guanine PC structures are closer to each other, while in the excited state they attain a square lattice structure, which results in a shift in the reflected color of the body.[220]

9. Conclusion

Detection of biomolecules at the POC faces multiple challenges, including the lack of centralized labs, limited technical capabilities, the absence of skilled staff, and poor health care management systems (particularly in resource-limited settings). PC-based biosensors represent a novel class of advanced optical biosensors that readily address these drawbacks. PC structures are used as biosensors for cells, bacteria, viruses, and numerous biomolecules, such as proteins, cancer biomarkers, allergens, DNAs, RNAs, glucose, and toxins. These structures can be manufactured with metals, oxides, plastics, polymers, and glass in mass quantities using NIL technology or wet chemical synthesis of colloidal and polymer structures. Recently, PC structures have been integrated with emerging technologies such as smartphones, flexible materials, and wearable sensors to enhance their utilization as potential diagnostic tools at the POC. However, clinical specimens may require sample preparation steps such as filtration, which may limit the use of PC-based biosensors at the POC. Additionally, complex biological fluids comprising cells and tissues may interfere with the transducer of biosensors and some of the delicate PC structures might experience challenges with the sensing mechanism including read-out systems. In addition, PC structures have been translated to a few products in biosensing, chemical and humidity sensing. PC-based biosensors represent a new class of advanced technology products that can be good candidates for a wide array of applications at the POC.

Acknowledgements

U. D. is a founder of and has an equity interest in: (i) DxNow Inc., a company that is developing microfluidic and imaging technologies for point-of-care diagnostic solutions, and (ii) Koek Biotech, a company that is developing microfluidic *in vitro* fertilization (IVF) technologies for clinical solutions. U. D.'s interests were viewed and managed in accordance with the conflict of interest policies. U. D. would like to acknowledge National Institutes of Health (NIH) R01 A1093282, R01 GM108584, R01 DE02497101, NIH R01 AI120683.

References

1 R. Monošík, M. Streanský and E. Šturdík, *Acta Chim. Slovaca*, 2012, **5**, 109–120.
2 IUPAC, Gloss. Chem. terms used Biotechnol. (IUPAC Recomm. 1992), 1992, 148.
3 J. P. Chambers, B. P. Arulanandam, L. L. Matta, A. Weis and J. J. Valdes, *Curr. Issues Mol. Biol.*, 2008, **10**, 1–12.
4 J. Wang, C. Wu, N. Hu, J. Zhou, L. Du and P. Wang, *Biosensors*, 2012, **2**, 127–170.
5 L. Yang and R. Bashir, *Biotechnol. Adv.*, 2008, **26**, 135–150.
6 C. Lissandrello, F. Inci, M. Francom, M. R. Paul, U. Demirci and K. L. Ekinci, *Appl. Phys. Lett.*, 2014, **105**, 113701.
7 J. Xu, D. Suarez and D. S. Gottfried, *Anal. Bioanal. Chem.*, 2007, **389**, 1193–1199.
8 A. L. Washburn, M. S. Luchansky, A. L. Bowman and R. C. Bailey, *Anal. Chem.*, 2010, **82**, 69–72.
9 J. Kirsch, C. Siltanen, Q. Zhou, A. Revzin and A. Simonian, *Chem. Soc. Rev.*, 2013, **42**, 8733–8768.
10 S. Myung, P. T. Yin, C. Kim, J. Park, A. Solanki, P. I. Reyes, Y. Lu, K. S. Kim and K. B. Lee, *Adv. Mater.*, 2012, **24**, 6081–6087.
11 M. Ozsoz, A. Erdem, P. Kara, K. Kerman and D. Ozkan, *Electroanalysis*, 2003, **15**, 613–619.
12 M. Plebani, *Ann. Clin. Biochem.*, 2010, **47**, 101–110.
13 P. Bonini, M. Plebani, F. Ceriotti and F. Rubboli, *Clin. Chem.*, 2002, **48**, 691–698.
14 S. F. Cheung, S. K. L. Cheng and D. T. Kamei, *J. Lab. Autom.*, 2015, **20**, 316–333.
15 C. Briggs, J. Carter, S.-H. Lee, L. Sandhaus, R. Simon-Lopez and J.-L. Vives Corrons, and International Council for Standardization in Haematology (ICSH), *Int. J. Lab. Hematol.*, 2008, vol. 30, pp. 105–116.
16 S. D. Blacksell, R. G. Jarman, R. V. Gibbons, A. Tanganuchitcharnchai, M. P. Mammen, A. Nisalak, S. Kalayanarooj, M. S. Bailey, R. Premaratna, H. J. de Silva, N. P. J. Day and D. G. Lalloo, *Clin. Vaccine Immunol.*, 2012, **19**, 804–810.
17 J. W. Pickering, T. B. Martins, M. C. Schroder and H. R. Hill, *Clin. Diagn. Lab. Immunol.*, 2002, **9**, 872–876.
18 MarketsandMarkets, In Vitro Diagnostics (IVD) Market by Product (instruments, Reagents, Software, Service) Technology (Immunoassay, Clinical Chemistry, Molecular Diagnostics, Hematology) by Application (Diabetes, Cancer, Cardiology, Autoimmune Diseases) – Forecast to 2020, 2015.
19 S. Wang, F. Inci, G. De Libero, A. Singhal and U. Demirci, *Biotechnol. Adv.*, 2013, **31**, 438–449.
20 U. A. Gurkan, S. Moon, H. Geckil, F. Xu, S. Wang, T. J. Lu and U. Demirci, *Biotechnol. J.*, 2011, **6**, 138–149.
21 O. Tokel, F. Inci and U. Demirci, *Chem. Rev.*, 2014, **114**, 5728–5752.
22 H. Shafiee, S. Wang, F. Inci, M. Toy, T. J. Henrich, D. R. Kuritzkes and U. Demirci, *Annu. Rev. Med.*, 2015, **66**, 387–405.
23 S. Tasoglu, H. Cumhur Tekin, F. Inci, S. Knowlton, S. Q. Wang, F. Wang-Johanning, G. Johanning, D. Colevas and U. Demirci, *Proc. IEEE*, 2015, **103**, 161–178.
24 U. H. Yildiz, F. Inci, S. Wang, M. Toy, H. C. Tekin, A. Javaid, D. T.-Y. Lau and U. Demirci, *Biotechnol. Adv.*, 2015, **33**, 178–190.
25 W. Asghar, M. Yuksekkaya, H. Shafiee, M. Zhang, M. O. Ozen, F. Inci, M. Kocakulak and U. Demirci, *Sci. Rep.*, 2016, **6**, 21163.
26 A. T. Choko, N. Desmond, E. L. Webb, K. Chavula, S. Napierala-Mavedzenge, C. A. Gaydos, S. D. Makombe, T. Chunda, S. B. Squire, N. French, V. Mwapasa and E. L. Corbett, *PLoS Med.*, 2011, **8**, e1001102.
27 D. C. Mabey, K. A. Sollis, H. A. Kelly, A. S. Benzaken, E. Bitarakwate, J. Changalucha, X. S. Chen, Y. P. Yin, P. J. Garcia, S. Strasser, N. Chintu, T. Pang, F. Terris-Prestholt, S. Sweeney and R. W. Peeling, *PLoS Med.*, 2012, **9**, 8.

28 N. Engel, G. Ganesh, M. Patil, V. Yellappa, N. P. Pai, C. Vadnais and M. Pai, *PLoS One*, 2015, **10**, e0135112.
29 N. P. Pai, S. Wilkinson, R. Deli-Houssein, R. Vijh, C. Vadnais, T. Behlim, M. Steben, N. Engel and T. Wong, *Point Care*, 2015, **14**, 81–87.
30 P. B. Luppa, C. Müller, A. Schlichtiger and H. Schlebusch, *TrAC, Trends Anal. Chem.*, 2011, **30**, 887–898.
31 M. A. Lifson, M. O. Ozen, F. Inci, S. Wang, H. Inan, M. Baday, T. J. Henrich and U. Demirci, *Adv. Drug Delivery Rev.*, 2016, **103**, 90–104.
32 P. Yager, G. J. Domingo and J. Gerdes, *Annu. Rev. Biomed. Eng.*, 2008, **10**, 107–144.
33 D. Mabey, R. W. Peeling, A. Ustianowski and M. D. Perkins, *Nat. Rev. Microbiol.*, 2004, **2**, 231–240.
34 H. K. P. Mulder, A. Ymeti, V. Subramaniam and J. S. Kanger, *Opt. Express*, 2012, **20**, 20934–20950.
35 D. Dorfner, T. Zabel, T. Hürlimann, N. Hauke, L. Frandsen, U. Rant, G. Abstreiter and J. Finley, *Biosens. Bioelectron.*, 2009, **24**, 3688–3692.
36 F. Inci, U. Celik, B. Turken, H. Ö. Özer and F. N. Kok, *Biochem. Biophys. Reports*, 2015, **2**, 115–122.
37 F. Inci, C. Filippini, M. Baday, M. O. Ozen, S. Calamak, N. G. Durmus, S. Wang, E. Hanhauser, K. S. Hobbs, F. Juillard, P. P. Kuang, M. L. Vetter, M. Carocci, H. S. Yamamoto, Y. Takagi, U. H. Yildiz, D. Akin, D. R. Wesemann, A. Singhal, P. L. Yang, M. L. Nibert, R. N. Fichorova, D. T.-Y. Lau, T. J. Henrich, K. M. Kaye, S. C. Schachter, D. R. Kuritzkes, L. M. Steinmetz, S. S. Gambhir, R. W. Davis and U. Demirci, *Proc. Natl. Acad. Sci. U. S. A.*, 2015, **112**, E4354–4363.
38 F. Inci, O. Tokel, S. Wang, U. A. Gurkan, S. Tasoglu, D. R. Kuritzkes and U. Demirci, *ACS Nano*, 2013, **7**, 4733–4745.
39 H. Shafiee, M. Jahangir, F. Inci, S. Wang, R. Willenbrecht, F. F. Giguel, A. Tsibris, D. R. Kuritzkes and U. Demirci, *Small*, 2013, **9**, 2553–2563.
40 S. Viswanathan, T. N. Narayanan, K. Aran, K. D. Fink, J. Paredes, P. M. Ajayan, S. Filipek, P. Miszta, H. C. Tekin and F. Inci, *Mater. Today*, 2015, **18**, 513–522.
41 A. K. Yetisen, Y. Montelongo, F. da Cruz Vasconcellos, J. L. Martinez-Hurtado, S. Neupane, H. Butt, M. M. Qasim, J. Blyth, K. Burling, J. B. Carmody, M. Evans, T. D. Wilkinson, L. T. Kubota, M. J. Monteiro and C. R. Lowe, *Nano Lett.*, 2014, **14**, 3587–3593.
42 S. A. Asher and J. T. Baca, *Handbook Of Optical Sensing Of Glucose In Biological Fluids And Tissues*, 2009, pp. 387–417.
43 Z. Cai, J. T. Zhang, F. Xue, Z. Hong, D. Punihaole and S. A. Asher, *Anal. Chem.*, 2014, **86**, 4840–4847.
44 Q. Yan, J. Yu, Z. Cai and X. S. Zhao, *Hierarchically Structured Porous Materials*, 2011, pp. 531–576.
45 C. Fenzl, S. Wilhelm, T. Hirsch and O. S. Wolfbeis, *ACS Appl. Mater. Interfaces*, 2013, **5**, 173–178.
46 C. J. Choi and B. T. Cunningham, *Lab Chip*, 2007, **7**, 550–556.
47 Y. Nazirizadeh, U. Bog, S. Sekula, T. Mappes, U. Lemmer and M. Gerken, *Opt. Express*, 2010, **18**, 19120–19128.
48 V. N. Konopsky and E. V. Alieva, *Anal. Chem.*, 2007, **79**, 4729–4735.
49 X. Fan, I. M. White, S. I. Shopova, H. Zhu, J. D. Suter and Y. Sun, *Anal. Chim. Acta*, 2008, **620**, 8–26.
50 S. Xiao and N. A. Mortensen, *J. Eur. Opt. Soc.*, 2006, **1**, 06026.
51 P. Vukusic and J. R. Sambles, *Nature*, 2003, **424**, 852–855.
52 S. Kinoshita, S. Yoshioka and K. Kawagoe, *Proc. Biol. Sci.*, 2002, **269**, 1417–1421.
53 J. Zi, X. Yu, Y. Li, X. Hu, C. Xu, X. Wang, X. Liu and R. Fu, *Proc. Natl. Acad. Sci. U. S. A.*, 2003, **100**, 12576–12578.
54 C. Pouya, D. G. Stavenga and P. Vukusic, *Opt. Express*, 2011, **19**, 11355–11364.
55 R. C. McPhedran, N. A. Nicorovici, D. R. McKenzie, G. W. Rouse, L. C. Botten, V. Welch, A. R. Parker, M. Wohlgennant and V. Vardeny, *Phys. B*, 2003, **338**, 182–185.
56 F. Marlow, P. Sharifi, R. Brinkmann and C. Mendive, *Angew. Chem., Int. Ed.*, 2009, **48**, 6212–6233.
57 K. J. Vahala, *Nature*, 2003, **424**, 839–846.
58 P. Russell, *Science*, 2003, **299**, 358–362.
59 A. Di Falco, L. O'Faolain and T. F. Krauss, *Photonics Nanostruct. Fundam. Appl.*, 2008, **6**, 38–41.
60 J. N. Winn, Y. Fink, S. Fan and J. D. Joannopoulos, *Opt. Lett.*, 1998, **23**, 1573–1575.
61 C. Pacholski, *Sensors*, 2013, **13**, 4694–4713.
62 C. Jamois, R. B. Wehrspohn, L. C. Andreani, C. Hermann, O. Hess and U. Gösele, *Photonics Nanostruct. Fundam. Appl.*, 2003, **1**, 1–13.
63 D. Freeman, C. Grillet, M. W. Lee, C. L. C. Smith, Y. Ruan, A. Rode, M. Krolikowska, S. Tomljenovic-Hanic, C. M. de Sterke, M. J. Steel, B. Luther-Davies, S. Madden, D. J. Moss, Y.-H. Lee and B. J. Eggleton, *Photonics Nanostruct. Fundam. Appl.*, 2008, **6**, 3–11.
64 A. C. Edrington, A. M. Urbas, P. Derege, C. X. Chen, T. M. Swager, N. Hadjichristidis, M. Xenidou, L. J. Fetters, J. D. Joannopoulos, Y. Fink and E. L. Thomas, *Adv. Mater.*, 2001, **13**, 421–425.
65 L. Gonzalez-Urbina, K. Baert, B. Kolaric, J. Perez-Moreno and K. Clays, *Chem. Rev.*, 2012, **112**, 2268–2285.
66 M. G. Han, C. G. Shin, S. J. Jeon, H. Shim, C. J. Heo, H. Jin, J. W. Kim and S. Lee, *Adv. Mater.*, 2012, **24**, 6438–6444.
67 F. Meseguer, *Colloids Surf., A*, 2005, **270–271**, 1–7.
68 V. L. Colvin, *MRS Bull.*, 2001, **26**, 637–641.
69 J. MacLeod and F. Rosei, *Nat. Mater.*, 2013, **12**, 98–100.
70 S. Kim, A. N. Mitropoulos, J. D. Spitzberg, H. Tao, D. L. Kaplan and F. G. Omenetto, *Nat. Photonics*, 2012, **6**, 818–823.
71 Y. Y. Diao, X. Y. Liu, G. W. Toh, L. Shi and J. Zi, *Adv. Funct. Mater.*, 2013, **23**, 5373–5380.
72 J. H. Kang, J. H. Moon, S. K. Lee, S. G. Park, S. G. Jang, S. Yang and S. M. Yang, *Adv. Mater.*, 2008, **20**, 3061–3065.
73 K. Liu, T. A. Schmedake and R. Tsu, *A comparative study of colloidal silica spheres: photonic crystals versus Bragg's law*, 2008, vol. 372.
74 A. Rogach, A. Susha, F. Caruso, G. Sukhorukov, A. Kornowski, S. Kershaw, H. Möhwald, A. Eychmüller and H. Weller, *Adv. Mater.*, 2000, **12**, 333–337.
75 J. Zhang, Z. Sun and B. Yang, *Curr. Opin. Colloid Interface Sci.*, 2009, **14**, 103–114.

76 D. J. Norris, E. G. Arlinghaus, L. Meng, R. Heiny and L. E. Scriven, *Adv. Mater.*, 2004, **16**, 1393–1399.
77 C. Reese, C. Guerrero, J. Weissman, K. Lee and S. Asher, *J. Colloid Interface Sci.*, 2000, **232**, 76–80.
78 C. López, *Adv. Mater.*, 2003, **15**, 1679–1704.
79 J. Kouba, M. Kubenz, A. Mai, G. Ropers, W. Eberhardt and B. Loechel, *J. Phys.: Conf. Ser.*, 2006, **34**, 897–903.
80 Q.-C. Hsu, J.-J. Hsiao, T.-L. Ho and C.-D. Wu, *Microelectron. Eng.*, 2012, **91**, 178–184.
81 J. D. Joannopoulos, S. G. Johnson, J. N. Winn and R. D. Meade, *Photonic Crystals: Molding the Flow of Light*, Princeton University Press, 2008.
82 Y.-H. Lee and H. Y. Ryu, *IEEE Circuits Devices Mag.*, 2002, **18**, 8–15.
83 R. Magnusson and Y. Ding, in *Optical Science and Technology, SPIE's 48th Annual Meeting*, International Society for Optics and Photonics, 2003.
84 Z. S. Liu, S. Tibuleac, D. Shin, P. P. Young and R. Magnusson, *Opt. Lett.*, 1998, **23**, 1556.
85 S. S. Wang and R. Magnusson, *Appl. Opt.*, 1993, **32**, 2606–2613.
86 I. D. Block, N. Ganesh, M. Lu and B. T. Cunningham, *IEEE Sens. J.*, 2008, **8**, 274–280.
87 J. T. Zhang, L. Wang, J. Luo, A. Tikhonov, N. Kornienko and S. A. Asher, *J. Am. Chem. Soc.*, 2011, **133**, 9152–9155.
88 C. Fenzl, T. Hirsch and O. S. Wolfbeis, *Angew. Chem., Int. Ed.*, 2014, **53**, 3318–3335.
89 A. Di Falco, L. O'Faolain and T. F. Krauss, *Appl. Phys. Lett.*, 2009, **94**, 063503.
90 A. M. Cubillas, S. Unterkofler, T. G. Euser, B. J. M. Etzold, A. C. Jones, P. J. Sadler, P. Wasserscheid and P. S. J. Russell, *Chem. Soc. Rev.*, 2013, **42**, 8629.
91 H. Shafiee, E. Lidstone, M. Jahangir, F. Inci, E. Hanhauser, T. J. Henrich, D. R. Kuritzkes, B. T. Cunningham and U. Demirci, *Sci. Rep.*, 2014, **4**, 4116.
92 S. Pal, A. R. Yadav, M. A. Lifson, J. E. Baker, P. M. Fauchet and B. L. Miller, *Biosens. Bioelectron.*, 2013, **44**, 229–234.
93 T. Endo, S. Ozawa, N. Okuda, Y. Yanagida, S. Tanaka and T. Hatsuzawa, *Sens. Actuators, B*, 2010, **148**, 269–276.
94 M. F. Pineda, L. L.-Y. Chan, T. Kuhlenschmidt, C. J. Choi, M. Kuhlenschmidt and B. T. Cunningham, *IEEE Sens. J.*, 2009, **9**, 470–477.
95 C. Wu and S. Alvarez, *SPIE Defense, Security, and Sensing, International Society for Optics and Photonics*, 2009, vol. 7167.
96 N. Li, X. R. Cheng, A. Brahmendra, A. Prashar, T. Endo, C. Guyard, M. Terebiznik and K. Kerman, *Biosens. Bioelectron.*, 2013, **41**, 354–358.
97 S. O. Meade, M. Y. Chen, M. J. Sailor and G. M. Miskelly, *Anal. Chem.*, 2009, **81**, 2618–2625.
98 V. Toccafondo, J. García-Rupérez, M. J. Bañuls, A. Griol, J. G. Castelló, S. Peransi-Llopis and A. Maquieira, *Opt. Lett.*, 2010, **35**, 3673–3675.
99 F. Fleischhaker, A. C. Arsenault, F. C. Peiris, V. Kitaev, I. Manners, R. Zentel and G. A. Ozin, *Adv. Mater.*, 2006, **18**, 2387–2391.
100 B. Zhang, S. Dallo, R. Peterson, S. Hussain, T. Weitao and J. Y. Ye, *J. Biomed. Opt.*, 2011, **16**, 127006.
101 H. Zhang, Z. Jia, X. Lv, J. Zhou, L. Chen, R. Liu and J. Ma, *Biosens. Bioelectron.*, 2013, **44**, 89–94.
102 A. C. Sharma, T. Jana, R. Kesavamoorthy, L. Shi, M. A. Virji, D. N. Finegold and S. A. Asher, *J. Am. Chem. Soc.*, 2004, **126**, 2971–2977.
103 K. A. Kilian, L. M. H. Lai, A. Magenau, S. Cartland, T. Böcking, N. Di Girolamo, M. Gal, K. Gaus and J. J. Gooding, *Nano Lett.*, 2009, **9**, 2021–2025.
104 Y. Hu, X. Jiang, L. Zhang, J. Fan and W. Wu, *Biosens. Bioelectron.*, 2013, **48**, 94–99.
105 M. Ben-Moshe, V. L. Alexeev and S. A. Asher, *Anal. Chem.*, 2006, **78**, 5149–5157.
106 V. L. Alexeev, A. C. Sharma, A. V. Goponenko, S. Das, I. K. Lednev, C. S. Wilcox, D. N. Finegold and S. A. Asher, *Anal. Chem.*, 2003, **75**, 2316–2323.
107 B. Guan, A. Magenau, K. A. Kilian, S. Ciampi, K. Gaus, P. J. Reece and J. J. Gooding, *Faraday Discuss.*, 2011, **149**, 301–317; discussion 333–356.
108 P. Sharma, S. K. Roy and P. Sharan, in *IEEE TENSYMP 2014 – 2014 IEEE Region 10 Symposium*, 2014, pp. 171–176.
109 J. H. Han, H. J. Kim, L. Sudheendra, S. J. Gee, B. D. Hammock and I. M. Kennedy, *Anal. Chem.*, 2013, **85**, 3104–3109.
110 Y. Tan, J. F. Halsey, T. Tang, S. Vande Wetering, E. Taine, M. Van Cleve and B. T. Cunningham, *Biosens. Bioelectron.*, 2016, **77**, 194–201.
111 M. Baday, S. Calamak, N. G. Durmus, R. W. Davis, L. M. Steinmetz and U. Demirci, *Small*, 2015, **12**, 1222–1229.
112 U. A. Gurkan, S. Tasoglu, D. Akkaynak, O. Avci, S. Unluisler, S. Canikyan, N. MacCallum and U. Demirci, *Adv. Healthcare Mater.*, 2012, **1**, 661–668.
113 V. Mani, S. Wang, F. Inci, G. De Libero, A. Singhal and U. Demirci, *Adv. Drug Delivery Rev.*, 2014, **78**, 105–117.
114 W. G. Lee, Y.-G. Kim, B. G. Chung, U. Demirci and A. Khademhosseini, *Adv. Drug Delivery Rev.*, 2010, **62**, 449–457.
115 H. Shafiee, W. Asghar, F. Inci, M. Yuksekkaya, M. Jahangir, M. H. Zhang, N. G. Durmus, U. A. Gurkan, D. R. Kuritzkes and U. Demirci, *Sci. Rep.*, 2015, **5**, 8719.
116 S. Wang, M. A. Lifson, F. Inci, L.-G. Liang, Y.-F. Sheng and U. Demirci, *Expert Rev. Mol. Diagn.*, 2016, **16**, 449–459.
117 S. Wang, F. Inci, T. L. Chaunzwa, A. Ramanujam, A. Vasudevan, S. Subramanian, A. C. Fai Ip, B. Sridharan, U. A. Gurkan and U. Demirci, *Int. J. Nanomed.*, 2012, **7**, 2591–2600.
118 S. Wang, M. Esfahani, U. A. Gurkan, F. Inci, D. R. Kuritzkes and U. Demirci, *Lab Chip*, 2012, **12**, 1508–1515.
119 B. R. Schudel, C. J. Choi, B. T. Cunningham and P. J. A. Kenis, *Lab Chip*, 2009, **9**, 1676–1680.
120 S. Wang, S. Tasoglu, P. Z. Chen, M. Chen, R. Akbas, S. Wach, C. I. Ozdemir, U. A. Gurkan, F. F. Giguel, D. R. Kuritzkes and U. Demirci, *Sci. Rep.*, 2014, **4**, 3796.
121 A. K. Yetisen, M. S. Akram and C. R. Lowe, *Lab Chip*, 2013, **13**, 2210–2251.

122 X. Fan and I. M. White, *Nat. Photonics*, 2011, **5**, 591–597.
123 W. Shen, M. Li, L. Xu, S. Wang, L. Jiang, Y. Song and D. Zhu, *Biosens. Bioelectron.*, 2011, **26**, 2165–2170.
124 M. G. Scullion, A. Di Falco and T. F. Krauss, *Biosens. Bioelectron.*, 2011, **27**, 101–105.
125 M. G. Scullion, T. F. Krauss and A. Di Falco, *Sensors*, 2013, **13**, 3675–3710.
126 D. Zhang and Q. Liu, *Biosens. Bioelectron.*, 2016, **75**, 273–284.
127 A. K. Yetisen, J. L. Martinez-Hurtado, F. da Cruz Vasconcellos, M. C. E. Simsekler, M. S. Akram and C. R. Lowe, *Lab Chip*, 2014, **14**, 833–840.
128 A. S. M. Mosa, I. Yoo and L. Sheets, *BMC Med. Inf. Decis. Making*, 2012, **12**, 67.
129 P.-S. Liang, T. S. Park and J.-Y. Yoon, *Sci. Rep.*, 2014, **4**, 1–8.
130 T. S. Park, W. Li, K. E. K. McCracken and J. J.-Y. Yoon, *Lab Chip*, 2013, **22**, 256–258.
131 M. Zangheri, L. Cevenini, L. Anfossi, C. Baggiani, P. Simoni, F. Di Nardo and A. Roda, *Biosens. Bioelectron.*, 2015, **64**, 63–68.
132 V. Oncescu, D. O'Dell and D. Erickson, *Lab Chip*, 2013, **13**, 3232–3238.
133 A. Roda, E. Michelini, M. Zangheri, M. Di Fusco, D. Calabria and P. Simoni, *TrAC, Trends Anal. Chem.*, 2015, **79**, 317–325.
134 A. C. Sobieranski, F. Inci, H. C. Tekin, M. Yuksekkaya, E. Comunello, D. Cobra, A. von Wangenheim and U. Demirci, *Light: Sci. Appl.*, 2015, **4**, e346.
135 D. Gallegos, K. D. Long, H. Yu, P. P. Clark, Y. Lin, S. George, P. Nath and B. T. Cunningham, *Lab Chip*, 2013, **13**, 2124–2132.
136 S. Jahns, M. Bräu, B.-O. Meyer, T. Karrock, S. B. Gutekunst, L. Blohm, C. Selhuber-Unkel, R. Buhmann, Y. Nazirizadeh and M. Gerken, *Biomed. Opt. Express*, 2015, **6**, 3724–3736.
137 W. Tao, T. Liu, R. Zheng and H. Feng, *Sensors*, 2012, **12**, 2255–2283.
138 O. Olguin, P. A. Gloor and A. Pentland, *Proc. IEEE*, 2009, **66**, 1–4.
139 G. Appelboom, E. Camacho, M. E. Abraham, S. S. Bruce, E. L. Dumont, B. E. Zacharia, R. D'Amico, J. Slomian, J. Y. Reginster, O. Bruyère and E. S. Connolly, *Arch. Public Health*, 2014, **72**, 28.
140 N. Luo, J. Ding, N. Zhao, B. H. K. Leung and C. C. Y. Poon, in Proceedings – 11th International Conference on Wearable and Implantable Body Sensor Networks, BSN 2014, 2014, pp. 87–91.
141 S. Yao and Y. Zhu, *Nanoscale*, 2014, **6**, 2345.
142 D. Vilela, A. Romeo and S. Sánchez, *Lab Chip*, 2016, **16**, 402–408.
143 M. Caldara, C. Colleoni, E. Guido, G. Rosace, V. Re and A. Vitali, in *2013 IEEE International Conference on Body Sensor Networks, BSN 2013*, 2013, pp. 1–6.
144 A. J. Bandodkar and J. Wang, *Trends Biotechnol.*, 2014, **32**, 363–371.
145 L. Florea and D. Diamond, *Sens. Actuators, B*, 2015, **211**, 403–418.
146 X. Xu, H. Subbaraman, S. Chakravarty, A. Hosseini, J. Covey, Y. Yu, D. Kwong, Y. Zhang, W.-C. Lai, Y. Zou, N. Lu and R. T. Chen, *ACS Nano*, 2014, **8**, 12265–12271.
147 L. M. Fortes, M. C. Gonçalves and R. M. Almeida, *Opt. Mater.*, 2011, **33**, 408–412.
148 D. K. Cullen, Y. Xu, D. V Reneer, K. D. Browne, J. W. Geddes, S. Yang and D. H. Smith, *NeuroImage*, 2011, **54**(suppl 1), S37–S44.
149 D. K. Cullen, K. D. Browne, Y. Xu, S. Adeeb, J. A. Wolf, R. M. McCarron, S. Yang, M. Chavko and D. H. Smith, *J. Neurotrauma*, 2011, **28**, 2307–2318.
150 E. Mastronardi, A. Foster, X. Zhang and M. DeRosa, *Sensors*, 2014, **14**, 3156–3171.
151 R. Verma, R. R. Adhikary and R. Banerjee, *Lab Chip*, 2016, **16**, 1978–1992.
152 M. C. Chiappelli and R. C. Hayward, *Adv. Mater.*, 2012, **24**, 6100–6104.
153 A. K. Yetisen, H. Butt and S.-H. Yun, *ACS Sens.*, 2016, **1**, 493–497.
154 Z. Cai, L. A. Luck, D. Punihaole, J. D. Madura and S. A. Asher, *Chem. Sci.*, 2016, **49**, 1993–2007.
155 H. Yang, H. Liu, H. Kang and W. Tan, *J. Am. Chem. Soc.*, 2008, **130**, 6320–6321.
156 K. I. MacConaghy, D. M. Chadly, M. P. Stoykovich and J. L. Kaar, *Analyst*, 2015, **140**, 6354–6362.
157 E. Choi, Y. Choi, Y. H. P. Nejad, K. Shin and J. Park, *Sens. Actuators, B*, 2013, **180**, 107–113.
158 K. I. Macconaghy, C. I. Geary, J. L. Kaar and M. P. Stoykovich, *J. Am. Chem. Soc.*, 2014, **136**, 6896–6899.
159 M. K. Maurer, S. E. Gould and P. J. Scott, *Sens. Actuators, B*, 2008, **134**, 736–742.
160 B. Maeng, Y. Park and J. Park, *RSC Adv.*, 2016, **6**, 7384–7390.
161 X. Hu, J. Huang, W. Zhang, M. Li, C. Tao and G. Li, *Adv. Mater.*, 2008, **20**, 4074–4078.
162 J. Huang, C. Tao, Q. An, C. Lin, X. Li, D. Xu, Y. Wu, X. Li, D. Shen and G. Li, *Chem. Commun.*, 2010, **46**, 4103–4105.
163 J. Huang, C.-A. Tao, Q. An, W. Zhang, Y. Wu, X. Li, D. Shen and G. Li, *Chem. Commun.*, 2010, **46**, 967–969.
164 J. Ren, H. Xuan, C. Liu, C. Yao, Y. Zhu, X. Liu and L. Ge, *RSC Adv.*, 2015, **5**, 77211–77216.
165 K. V. Sreekanth, S. Zeng, K. T. Yong and T. Yu, *Sens. Actuators, B*, 2013, **182**, 424–428.
166 K. Kempa, B. Kimball, J. Rybczynski, Z. P. Huang, P. F. Wu, D. Steeves, M. Sennett, M. Giersig, D. V. G. L. N. Rao, D. L. Carnahan, D. Z. Wang, J. Y. Lao, W. Z. Li and Z. F. Ren, *Nano Lett.*, 2003, **3**, 13–18.
167 H. Butt, Q. Dai, T. D. Wilkinson and G. A. J. Amaratunga, *Photonics Nanostruct. Fundam. Appl.*, 2012, **10**, 499–505.
168 H. Butt, A. K. Yetisen, R. Ahmed, S. H. Yun and Q. Dai, *Appl. Phys. Lett.*, 2015, **106**, 121108.
169 R. Ahmed, A. A. Rifat, A. K. Yetisen, Q. Dai, S. H. Yun and H. Butt, *J. Appl. Phys.*, 2016, **119**, 113105.
170 A. I. Aristov, M. Manousidaki, A. Danilov, K. Terzaki, C. Fotakis, M. Farsari and A. V. Kabashin, *Sci. Rep.*, 2016, **6**, 25380.

171 K. V. Sreekanth, Y. Alapan, M. ElKabbash, E. Ilker, M. Hinczewski, U. A. Gurkan, A. De Luca and G. Strangi, *Nat. Mater.*, 2016, **15**, 621–627.
172 P. V. Parimi, W. T. Lu, P. Vodo and S. Sridhar, *Nature*, 2003, **426**, 404.
173 L. L. Chan, M. Pineda, J. T. Heeres, P. J. Hergenrother and B. T. Cunningham, *ACS Chem. Biol.*, 2008, **3**, 437–448.
174 N. Skivesen, A. Têtu, M. Kristensen, J. Kjems, L. H. Frandsen and P. I. Borel, *Opt. Express*, 2007, **15**, 3169.
175 M. R. Lee and P. M. Fauchet, *Opt. Express*, 2007, **15**, 4530.
176 A. L. Washburn, L. C. Gunn and R. C. Bailey, *Anal. Chem.*, 2009, **81**, 9499–9506.
177 S. Zlatanovic, L. W. Mirkarimi, M. M. Sigalas, M. A. Bynum, E. Chow, K. M. Robotti, G. W. Burr, S. Esener and A. Grot, *Sens. Actuators, B*, 2009, **141**, 13–19.
178 M. M. Orosco, C. Pacholski, G. M. Miskelly and M. J. Sailor, *Adv. Mater.*, 2006, **18**, 1393–1396.
179 M. Cretich, D. Breda, F. Damin, M. Borghi, L. Sola, S. M. Unlu, S. E. Burastero and M. Chiari, *Anal. Bioanal. Chem.*, 2010, **398**, 1723–1733.
180 I. Skrindo, C. Lupinek, R. Valenta, V. Hovland, S. Pahr, A. Baar, K.-H. Carlsen, P. Mowinckel, M. Wickman, E. Melen, J. Bousquet, J. M. Anto and K. C. Lødrup Carlsen, *Pediatr. Allergy Immunol.*, 2015, **26**, 239–246.
181 A. Pokhriyal, M. Lu, V. Chaudhery, C.-S. Huang, S. Schulz and B. T. Cunningham, *Opt. Express*, 2010, **18**, 24793–24808.
182 A. M. Caliendo, D. N. Gilbert, C. C. Ginocchio, K. E. Hanson, L. May, T. C. Quinn, F. C. Tenover, D. Alland, A. J. Blaschke, R. A. Bonomo, K. C. Carroll, M. J. Ferraro, L. R. Hirschhorn, W. P. Joseph, T. Karchmer, A. T. MacIntyre, L. B. Reller and A. F. Jackson, *Clin. Infect. Dis.*, 2013, **57**(suppl 3), S139–S170.
183 R. J. Trent, *Molecular medicine: genomics to personalized healthcare*, Academic Press, 2005.
184 Q. Jiang, T. Turner, M. X. Sosa, A. Rakha, S. Arnold and A. Chakravarti, *Hum. Mutat.*, 2012, **33**, 281–289.
185 H. J. Chung, C. M. Castro, H. Im, H. Lee and R. Weissleder, *Nat. Nanotechnol.*, 2013, **8**, 369–375.
186 A. J. Qavi, J. T. Kindt, M. A. Gleeson and R. C. Bailey, *Anal. Chem.*, 2011, **83**, 5949–5956.
187 E. Jankowsky and M. E. Harris, *Nat. Rev. Mol. Cell Biol.*, 2015, **16**, 533–544.
188 M. Li, F. He, Q. Liao, J. Liu, L. Xu, L. Jiang, Y. Song, S. Wang and D. Zhu, *Angew. Chem., Int. Ed. Engl.*, 2008, **47**, 7258–7262.
189 S. Chakravarty, W.-C. Lai, Y. Zou, H. A. Drabkin, R. M. Gemmill, G. R. Simon, S. H. Chin and R. T. Chen, *Biosens. Bioelectron.*, 2013, **43**, 50–55.
190 U. S. Dinish, G. Balasundaram, Y. T. Chang and M. Olivo, *J. Biophotonics*, 2014, **7**, 956–965.
191 S. Padmanabhan, V. K. Shinoj, V. M. Murukeshan and P. Padmanabhan, *J. Biomed. Opt.*, 2010, **15**, 017005.
192 F. Liang, N. Clarke, P. Patel, M. Loncar and Q. Quan, *Opt. Express*, 2013, **21**, 32306–32312.
193 C.-S. Huang, V. Chaudhery, A. Pokhriyal, S. George, J. Polans, M. Lu, R. Tan, R. C. Zangar and B. T. Cunningham, *Anal. Chem.*, 2012, **84**, 1126–1133.
194 H. Mukundan, A. S. Anderson, W. K. Grace, K. M. Grace, N. Hartman, J. S. Martinez and B. I. Swanson, *Sensors*, 2009, **9**, 5783–5809.
195 S. Mandal, R. Akhmechet, L. Chen, S. Nugen, A. Baeumner and D. Erickson, *Nanoeng. Fabr. Prop. Opt. Devices IV*, 2007, **6645**, J6451.
196 G. Deng, K. Xu, Y. Sun, Y. Chen, T. Zheng and J. Li, *Anal. Chem.*, 2013, **85**, 2833–2840.
197 H. Kolb and T. Mandrup-Poulsen, *Diabetologia*, 2010, **53**, 10–20.
198 T. Scully, *Nature*, 2012, **485**, S2–S3.
199 S. K. Vashist, *Anal. Chim. Acta*, 2012, **750**, 16–27.
200 A. J. Bandodkar, W. Jia, C. Yardimci, X. Wang, J. Ramirez and J. Wang, *Anal. Chem.*, 2015, **87**, 394–398.
201 A. K. Yetisen, H. Butt, F. da Cruz Vasconcellos, Y. Montelongo, C. A. B. Davidson, J. Blyth, L. Chan, J. B. Carmody, S. Vignolini, U. Steiner, J. J. Baumberg, T. D. Wilkinson and C. R. Lowe, *Adv. Opt. Mater.*, 2014, **2**, 250–254.
202 E. Coscelli, M. Sozzi, F. Poli, D. Passaro, A. Cucinotta, S. Selleri, R. Corradini and R. Marchelli, *IEEE J. Sel. Top. Quantum Electron.*, 2010, **16**, 967–972.
203 T. Ding, F. Wang, K. Song, G. Yang and C.-H. Tung, *J. Am. Chem. Soc.*, 2010, **132**, 17340–17342.
204 C. Kang, C. T. Phare, Y. A. Vlasov, S. Assefa and S. M. Weiss, *Opt. Express*, 2010, **18**, 27930–27937.
205 W. Libaers, B. Kolaric, R. A. L. Vallée, J. E. Wong, J. Wouters, V. K. Valev, T. Verbiest and K. Clays, in *SPIE Optical Engineering + Applications*, International Society for Optics and Photonics, 2009, p. 74670C.
206 C. E. Chivers, E. Crozat, C. Chu, V. T. Moy, D. J. Sherratt and M. Howarth, *Nat. Methods*, 2010, **7**, 391–393.
207 D. M. Yebra, S. Kiil and K. Dam-Johansen, *Prog. Org. Coat.*, 2004, **50**, 75–104.
208 I. Banerjee, R. C. Pangule and R. S. Kane, *Adv. Mater.*, 2011, **23**, 690–718.
209 Y.-S. Sun, *J. Lab. Autom.*, 2015, **20**, 334–353.
210 Y. S. Sun, J. P. Landry, Y. Y. Fei, X. D. Zhu, J. T. Luo, X. B. Wang and K. S. Lam, *Langmuir*, 2008, **24**, 13399–13405.
211 R. Chauhan, J. Singh, T. Sachdev, T. Basu and B. D. Malhotra, *Biosens. Bioelectron.*, 2016, **81**, 532–545.
212 P. Dak, A. Ebrahimi, V. Swaminathan, C. Duarte-Guevara, R. Bashir and M. A. Alam, *Biosensors*, 2016, **6**, 14.
213 P. Toren, E. Ozgur and M. Bayindir, *Lab Chip*, 2016, **16**, 2572–2595.
214 H. Im, H. Shao, Y. Il Park, V. M. Peterson, C. M. Castro, R. Weissleder and H. Lee, *Nat. Biotechnol.*, 2014, **32**, 490–495.
215 J. W. Ndieyira, N. Kappeler, S. Logan, M. A. Cooper, C. Abell, R. A. McKendry and G. Aeppli, *Nat. Nanotechnol.*, 2014, **9**, 225–232.
216 H. Shafiee, M. K. Kanakasabapathy, F. Juillard, M. Keser, M. Sadasivam, M. Yuksekkaya, E. Hanhauser, T. J. Henrich, D. R. Kuritzkes, K. M. Kaye and U. Demirci, *Sci. Rep.*, 2015, **5**, 9919.

217 Transparency Market Research, Global Biosensors Market to Reach US$21.6 bn by 2020 owing to Growing Need for Monitoring Environmental Pollutants.
218 M. Christiansen, T. Bailey, E. Watkins, D. Liljenquist, D. Price, K. Nakamura, R. Boock and T. Peyser, *Diabetes Technol. Ther.*, 2013, **15**, 881–888.
219 S. P. Nichols, A. Koh, W. L. Storm, J. H. Shin and M. H. Schoenfisch, *Chem. Rev.*, 2013, **113**, 2528–2549.
220 J. Teyssier, S. V. Saenko, D. van der Marel and M. C. Milinkovitch, *Nat. Commun.*, 2015, **6**, 6368.
221 J. O. Grepstad, P. Kaspar, O. Solgaard, I.-R. Johansen and A. S. Sudbø, *Opt. Express*, 2012, **20**, 7954–7965.
222 S. Lin, J. Hu, L. Kimerling and K. Crozier, *Opt. Lett.*, 2009, **34**, 3451–3453.
223 S. Mandal, X. Serey and D. Erickson, *Nano Lett.*, 2010, **10**, 99–104.
224 M. R. Lee and P. M. Fauchet, *Opt. Lett.*, 2007, **32**, 3284.
225 K. Liu and L. Jiang, *Nano Today*, 2011, **6**, 155–175.
226 Y. Zhao, X. Zhao and Z. Gu, *Adv. Funct. Mater.*, 2010, **20**, 2970–2988.
227 V. Chaudhery, S. George, M. Lu, A. Pokhriyal and B. T. Cunningham, *Sensors*, 2013, **13**, 5561–5584.
228 I. Mukherjee, G. Hajisalem and R. Gordon, *Opt. Express*, 2011, **19**, 22462–22469.
229 S. Saito, F. Y. Gardes, A. Z. Al-attili, K. Tani, K. Oda, Y. Suwa, T. Ido, Y. Ishikawa, S. Kako and S. Iwamoto, *Front. Mater.*, 2014, **1**, 1–15.
230 M. E. Calvo, S. Colodrero, N. Hidalgo, G. Lozano, C. López-López, O. Sánchez-Sobrado and H. Míguez, *Energy Environ. Sci.*, 2011, **4**, 4800.
231 K. K. Seet, V. Mizeikis, S. Matsuo, S. Juodkazis and H. Misawa, *Adv. Mater.*, 2005, **17**, 541–545.
232 J.-H. Lee, C.-H. Kim, K.-M. Ho and K. Constant, *Adv. Mater.*, 2005, **17**, 2481–2485.
233 Y. A. Vlasov, X. Z. Bo, J. C. Sturm and D. J. Norris, *Nature*, 2001, **414**, 289–293.
234 S. George, V. Chaudhery, M. Lu, M. Takagi, N. Amro, A. Pokhriyal, Y. Tan, P. Ferreira and B. T. Cunningham, *Lab Chip*, 2013, **13**, 4053–4064.
235 U. S. Dinish, C. Y. Fu, K. S. Soh, B. Ramaswamy, A. Kumar and M. Olivo, *Biosens. Bioelectron.*, 2012, **33**, 293–298.
236 E. Chow, A. Grot, L. W. Mirkarimi, M. Sigalas and G. Girolami, *Opt. Lett.*, 2004, **29**, 1093–1095.
237 S. Chakravarty, Y. Zou, W.-C. Lai and R. T. Chen, *Biosens. Bioelectron.*, 2012, **38**, 170–176.
238 J. García-Rupérez, V. Toccafondo, M. J. Bañuls, J. G. Castelló, A. Griol, S. Peransi-Llopis and Á. Maquieira, *Opt. Express*, 2010, **18**, 24276–24286.
239 N. Massad-Ivanir, G. Shtenberg and E. Segal, *Adv. Exp. Med. Biol.*, 2012, **733**, 37–45.
240 W.-C. Lai, S. Chakravarty, Y. Zou and R. T. Chen, *Opt. Lett.*, 2012, **37**, 1208–1210.
241 S. A. Asher, V. L. Alexeev, A. V. Goponenko, A. C. Sharma, I. K. Lednev, C. S. Wilcox and D. N. Finegold, *J. Am. Chem. Soc.*, 2003, **125**, 3322–3329.
242 M. Huang, A. A. Yanik, T.-Y. Chang and H. Altug, *Opt. Express*, 2009, **17**, 24224–24233.
243 W. Shen, M. Li, C. Ye, L. Jiang and Y. Song, *Lab Chip*, 2012, **12**, 3089–3095.
244 R. S. Gaster, D. A. Hall, C. H. Nielsen, S. J. Osterfeld, H. Yu, K. E. Mach, R. J. Wilson, B. Murmann, J. C. Liao, S. S. Gambhir and S. X. Wang, *Nat. Med.*, 2009, **15**, 1327–1332.

